Supplementary Materials
A novel computational approach for drug repurposing using systems biology

March 19, 2018

Contents

1 Overview

Some approaches [61, 107, 26] employ Over-Representation Analysis (ORA) in order to understand the mode of actions (MoA) of drugs and their potential new usages. The most recent approach [61], DGE-NET, is based on the hypothesis that drugs with similar binding patterns (to a reference target protein) have similar molecular activities. In step 1, drug-target interactions (drug-target signatures) are predicted. DGE-NET ranks drugs that most likely bind to a given target based on similarity scores between different drugs and the given target. To do this, a modified version of Train, Match, Fit and Streamline (TMFS) [33] is used. TMFS determines the binding potential of a protein-ligand complex incorporating docking, three-dimensional shape, and ligand physicochemical data. For a given protein target, the top 40 drugs (1% of all drugs) are selected as hits for the next step. In step 2, the associations between the drug-target signatures on the one hand, and diseases, pathways, functions, and protein-protein interactions on the other hand, are identified. To this end, a hypergeometric test is applied at different biological levels: protein targets, protein-protein interactions (PPIs), cell signaling pathways, and molecular functions. In this step, gene expression data of the given disease is exploited to identify differentially expressed genes by comparing the expression values of two groups of samples: normal and disease. DAVID [57, 56] and STRING analysis [38] is applied on the list of differentially expressed genes to indicate the associations at different levels (by computing z-scores). The identified associations are validated based on the current literatures and annotated databases. DGE-NET is applied to human disease gene expression datasets: rheumatoid arthritis, inflammatory bowel disease, Alzheimer's disease, and Parkinson's disease to prioritize FDA-approved drugs for repurposing purposes.

Another approach [107] performs the pathway enrichment analysis to investigate MoA and clinical functions of the FDA-approved drugs. First, it selects sixteen FDA-approved drugs (with available target information) from DrugBank [154]. Then, it retrieves primary and secondary targets of these drugs from MMDB [87], PubChem [80] and GEO datasets [36]. And finally, it applies the enrichment analysis based on a modified Fisher's Test using the drug targets and pathways data. Pathways are ranked based on the numbers of retrieved drug targets involved in each pathway. Pathways with p-values <0.05 are chosen for further investigations.

The third method using an ORA approach analyzes the associations among drugs, targets and biological functions [26]. It assigns drugs into nine classes based on their targets: (1) G protein-coupled receptors, (2) cytokine receptors, (3) nuclear receptors, (4) ion channels, (5) transporters, (6) enzymes, (7) protein kinases, (8) cellular antigens and (9) pathogens. Then, it employs an enrichment analysis to identify the associations between the drugs and features including GO terms [7] and KEGG (`http://www.genome.ad.jp/kegg/`) pathways. Thus,

given the drug and the KEGG pathway (or GO term), an enrichment score is computed as S_KEGG (or S_GO) based on the result of hypergeometric test (p-value). Overall, 279 KEGG pathways and 17,904 GO terms are exploited to obtain the enrichments scores. Each drug is represented by 279 S_KEGG enrichment scores and S_GO 17,904 enrichment scores. Finally, the feature selection minimum redundancy maximum relevance (mRMR) method [110] is used to extract the key features. Pathways and GO terms that are highly enriched by several classes of drugs can be investigated for drug interaction predictions. For instance, the neuroactive ligand-receptor interaction pathway is enriched with two classes: GPCR and IC. This suggests that drugs with different targets may belong to the same biological pathway, thus also suggesting a potential for synergistic drug interactions.

The lack of a unifying analysis at system-level makes such ORA methods limited.

In this study, we use: i) KEGG signaling pathways, ii) drug target data, and iii) disease associated genes to construct a global network with genes specific to the drug and disease of interest (called drug-disease network, DDN). We then measure gene perturbation signatures for drug-disease pairs by propagating measured expression changes across the network topology.

Figure 1 shows the DDN network constructed for Sunitinib, the proposed candidate for IPF. This network consists of 782 genes, including the Sunitinib target genes: CSF1, FLT(1,3,4), KDR, LYN, PDGFR(α,β), and IPF-associated gene SRC. Figure 2 focused on four genes (CSF1, KDR, PDGFRα, SRC) of this network, among which KDR, PDGFRα, SRC are also target genes of Nintedanib (FDA-approved drug for IPF). CSF1 is a source node (indegree=0) associated to 18 downstream genes, including KDR and PDGFRα through *PI3K-Akt signaling pathway*. Recent preclinical studies in IPF show that the antifibrotic effect of Nintedanib is associated with the inhibition of tyrosine phosphorylation on CSF1 receptor [145]. Another clinical study suggests the important role of CSF1 in the pathogenesis of pulmonary fibrosis both in mice and in patients with IPF through the contribution of mononuclear phagocytes and CCL2 production [9, 16]. In total, there are 39 genes directly upstream of SRC, including KDR and PDGFRα, which are incorporated in calculating the amount of perturbation for SRC.

Methods based on protein-protein interactions that employ over-representation analysis (ORA) are limited by the fact that each gene is analyzed independently without a unifying analysis at a system level, while the proposed approach aims to consider the system-level dependencies and interactions on the drug-disease-specific network. One of the existing approaches for drug repurposing is based on an over-representation analysis of various pathways, based on the genes targeted by a given drug [61]. Based on this approach, a drug is first associated with pathways based on its directly targeted genes. Using this approach, Sunitinib can be associated to the following KEGG pathways: *MAPK signaling pathway*, *Cytokine-cytokine receptor interaction*, *VEGF signaling pathway*, and *Pathways*

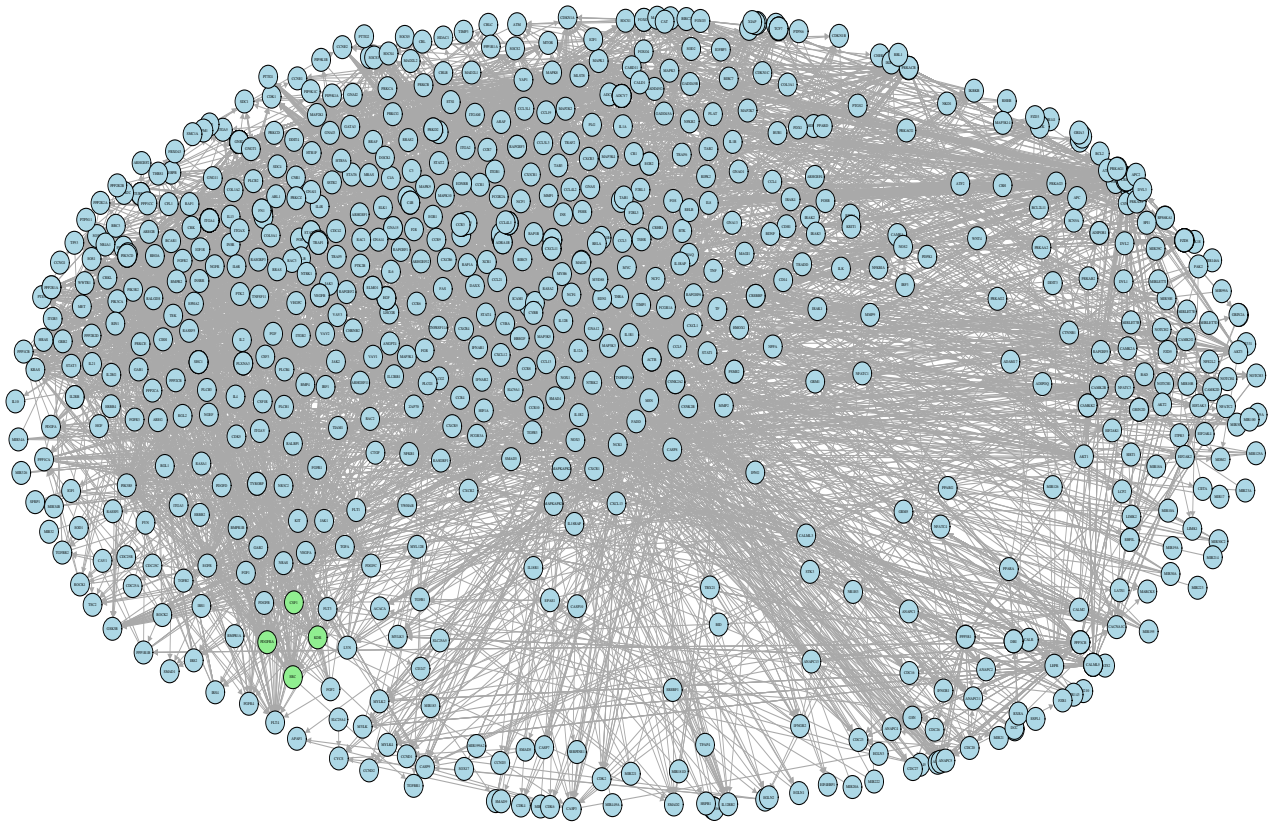

Figure 1: The DDN network constructed for Sunitinib, the proposed drug candidate for IPF.

in cancer. Subsequently, Issa *et al.* expand the set of genes to include the genes having direct interactions with the Sunitinib target genes using PPI data, and recalculated the pathways enriched in these "predicted targets". Table 1 shows the list of pathways that are significantly enriched in such predicted targets (FDR-corrected p-values less than 0.05). Although this type of ORA analysis could provide useful associations between Sunitinib and various pathways, extrapolating from pathways to diseases may not be optimal since there are many diseases that might be relevant to these pathways. For instance, the KEGG pathway *Pathways in cancer* is associated with over 1,000 diseases according to CTD [90] (list included in the supplementary files). This illustrates why this simple pathway-based enrichment approach cannot be used for effective drug repurposing and explains why our system-level analysis is able to provide much more specific results.

In summary, the limitations of these methods can be summarized as follows: i) the obtained target proteins might not be the exact target of a drug (for in-

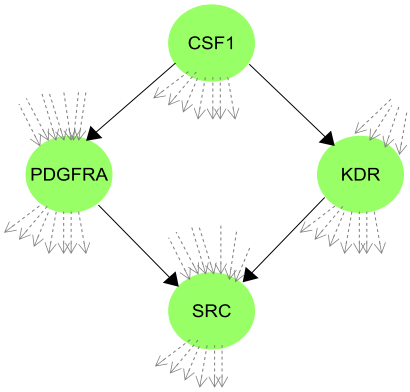

Figure 2: A subnetwork of DDN constructed for Sunitinib, the proposed drug candidate for IPF. PDGFRA, KDR, SRC are target genes of both Sunitinib and Nintedanib (FDA-approved drug for IPF), while CSF1 is targeted only by Sunitinib. Recent preclinical studies in IPF show that the antifibrotic effect of Nintedanib is associated with the inhibition of tyrosine phosphorylation on CSF1 receptor [145]. Another clinical study suggests the important role of CSF1 in the pathogenesis of pulmonary fibrosis both in mice and in patients with IPF through the contribution of mononuclear phagocytes and CCL2 production [9, 16]. In total, there are 39 genes directly upstream of SRC, including KDR and PDGFRα, which are incorporated in calculating the amount of perturbation for SRC.

Table 1: A list of pathways that are significantly enriched in predicted target genes for Sunitinib (FDR-corrected p-value < 0.05).

Pathway	pORA.fdr
PI3K-Akt signaling pathway	1.08E-18
Cytokine-cytokine receptor interaction	1.11E-15
Focal adhesion	2.80E-14
Pathways in cancer	1.20E-12
Melanoma	1.75E-07
Prostate cancer	8.30E-07
mTOR signaling pathway	1.08E-06
Gap junction	1.29E-05
MAPK signaling pathway	3.73E-05
Glioma	3.73E-05
HIF-1 signaling pathway	3.73E-05
Endocytosis	0.00088
Pertussis	0.00093
Regulation of actin cytoskeleton	0.00093
Rheumatoid arthritis	0.00174
Transcriptional misregulation in cancer	0.00317
Amoebiasis	0.00468
Legionellosis	0.00638
Acute myeloid leukemia	0.00747
p53 signaling pathway	0.00904
Long-term potentiation	0.00943
Hepatitis B	0.00982
HTLV-I infection	0.01044
Hypertrophic cardiomyopathy (HCM)	0.01341
Progesterone-mediated oocyte maturation	0.01341
Calcium signaling pathway	0.01605
Oocyte meiosis	0.02104
Osteoclast differentiation	0.04606
Amyotrophic lateral sclerosis (ALS)	0.04606
Insulin signaling pathway	0.04798

stance, they can be indirectly associated to the drug because of down or upstream proteins or cross-talk effects); ii) the target(s) of a drug have a limited ability to identify the pathways based on enrichment alone since one or a few genes on a pathway are unlikely to constitute sufficient statistical evidence; iii) the drug targets might be involved in variety of pathways that are not specifically related to the drug primary target. Thus such methods may fail in identifying significant pathways related to biological functions of the drug based on their target information.

Although existing drug repurposing methods showed moderate success, they are far from bringing critical advancements in the drug development pipeline. Most of these approaches rely only on an analysis of a set of differentially expressed genes. However, changes in genes expression are propagated in the system through a complex gene signaling network and this fact is not captured by approaches using only lists of DE genes [35, 95, 72].

It has been shown that many drugs exert their effect through modulation of several proteins rather than single targets [106, 54, 117, 106, 53]. Furthermore, the analysis by [162] shows that not all drugs directly impact the proteins associated with the root cause of a disease. These findings suggest that drug repurposing may be more successful if it used novel paradigms, going beyond lists of genes.

2 Materials and methods

2.1 Drug gene expression data

The drug data come from two different sources: i) Connectivity map (CMap) [78] ii) NIH's Library of Integrated Network-based Cellular Signatures (LINCS) (`http://www.lincsproject.org/`). In order to avoid any bias, we had to use four instances (with the highest number of DE genes) for any drugs that we consider from LINCS. The LINCS signature profiles are derived from comparing expression values of a small molecule to the control profiles (z-score with respect to vehicle control). For each gene, we calculate the p-value based on the z-score by using the normal distribution. We eliminate datasets that had fewer than 1% DE genes (FDR-corrected p-value < 0.05). In total, 260 datasets involving 65 distinct small molecules pass these criteria.

The CMap database has 6,100 gene expression profiles for 1,309 distinct small molecules measured on different cell lines. In order to take advantage of cell line diversity, in this work we used all cell lines. These profiles are pre-processed using the Robust Multi-chip Average (RMA) method [60]. Then, for each gene we use a moderated t-test [136] to calculate the p-value. We eliminate datasets that had fewer than 1% DE genes (FDR-corrected p-value < 0.05). Various drugs are represented by different number of instances. In order to avoid any bias related to the number of instances available for each drug, and because we have several

FDA-approved drugs for each condition, we select only instances with the highest number of DE genes for each drug (at most two instances). In total, 170 drug datasets involving 121 distinct small molecules pass these criteria.

We use two sources: i) Connectivity map (CMap) [78] for breast cancer and prostate cancer, and ii) NIH's Library of Integrated Network-based Cellular Signatures (LINCS) for idiopathic pulmonary fibrosis (IPF) and non-small cell lung cancer. We used two different data sources in order to show the approach is reliable and works independently of the source of the drug data. CMap database has several of FDA-approved drugs for breast cancer and prostate cancer but none for idiopathic pulmonary disease (IPF). So, for IPF we used LINCS database that has several gene expression profiles for Nintedanib (an FDA-aproved drug for IPF).

We chose to use LINCS for non-small cancer (NSCLC) rather than CMap for two reasons. First, more FDA-approved drugs belong to this database. (four drug instances for each of FDA-approved drugs: Gefitinib and Crizotinib). In comparison, the only FDA-approved drug for NSCLC in CMap is Paclitaxel and there is only one instance for this drug. Second, in LINCS, 123 out of 260 drug instances are measured on the A549 cell line that is the human lung adenocarcinoma epithelial cell line (a model For NSCLC). Since IPF is a chronic progressive and ultimately fatal disease that did not have any effective treatment until recently, we were interested to see if our proposed approach is able to predict any new treatments for this disease.

2.2 A systematic method to select the repurposing candidates

As we described in the manuscript, we used a systematic scoring and ranking method in order to select repurposing drug candidates for a given indication. As shown in Panel A of Figure 3, given a ranked-list of drugs (drug instances) obtained by applying our approach on a disease dataset, a score for drug $Drug_x$ is defined as $Score(Drug_x) = a - b$, where terms a and b denote the number of already FDA-approved drugs (gold standards) that are ranked worse and better than $Drug_x$, respectively. Panel B in this figure shows the computed scores for a number of top-ranked dugs from non-small cell lung cancer (NSCLC) results. In total, there are 8 FDA-approved drugs for NSCLC in our drug input list. For instance, the score assigned to GSM1740080_sunitinib for the GSE11969-adenocarcinoma dataset is 6, as there is only one FDA-approved drug (highlighted with green) ranked better than GSM1740080_sunitinib and there are 7 FDA-approved drugs ranked below it (7-1=6). A score of 8 means that each candidate ranked higher than all 8 instances of FDA-approved drugs.

Table II in Panel B summarizes the scores assigned to GSM1741743_sirolimus, GSM1738326_mocetinostat, and GSM1740080_sunitinib using 4 NSCLC datasets.

We then calculate an average score for each drug across different disease datasets, and different instances, if there are multiple instances for that drug. This is shown in Figure 4.

We select the top 5% of drugs ranked lists obtained by applying our approach on disease datasets and rank such drugs based on the scores computed by the systematic method, from highest to the lowest.

A

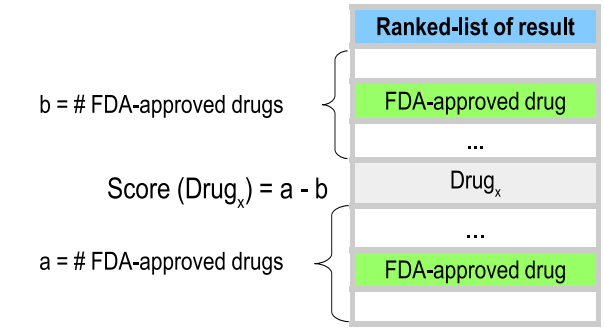

Table I

	GSE11969-adenocarcinoma	GSE11969-large cell carcinoma	GSE11969-squamous cell carcinoma	GSE32863-NSCLC
1	GSM1741743_sirolimus	GSM1741743_sirolimus	GSM1741743_sirolimus	GSM1741743_sirolimus
2	GSM1741104_sunitinib	GSM1741104_sunitinib	GSM1741104_sunitinib	GSM1738326_mocetinostat
3	GSM1738326_mocetinostat	GSM1739358_mocetinostat	GSM1740080_sunitinib	GSM1741104_sunitinib
4	GSM1739358_mocetinostat	GSM1738326_mocetinostat	GSM1738326_mocetinostat	GSM1740080_sunitinib
5	GSM1746613_enzastaurin	GSM1740080_sunitinib	GSM1746613_enzastaurin	GSM1739358_mocetinostat
6	GSM1742552_linifanib	GSM1741800_mitoxantrone	GSM1739358_mocetinostat	GSM1742878_dasatinib
7	GSM1742645_gefitinib	GSM1744393_gefitinib	GSM1744393_gefitinib	GSM1744393_gefitinib
8	GSM1740080_sunitinib	GSM1742645_gefitinib	GSM1742878_dasatinib	GSM1740301_ponatinib
9	GSM1737700_rucaparib	GSM1746613_enzastaurin	GSM1740081_sunitinib	GSM1740081_sunitinib
10	GSM1744393_gefitinib	GSM1742878_dasatinib	GSM1740917_saracatinib	GSM1742552_linifanib
...	...	...	...	...

B

Table II

	GSM1741743_sirolimus	GSM1738326_mocetinostat	GSM1740080_sunitinib
GSE11969-adenocarcinoma	8	8	6
GSE11969-large cell carcinoma	8	8	8
GSE11969-squamous cell carcinoma	8	8	8
GSE32863-NSCLC	8	8	8

Figure 3: A) Given a ranked-list of drugs (drug instances) obtained by applying our approach on a disease dataset, a score is assigned to each drug indicating how better or worse that drug is ranked in comparison to already FDA-approved drugs. The score for $Drug_x$ is defined as $Score(Drug_x) = a - b$, where a and b denote the number of already FDA-approved drugs that are ranked worse and better than $Drug_x$, respectively. B) The non-small cell lung cancer (NSCLC): in total there are 8 drugs that are already FDA-approved for treatment of NSCLC. Table I shows the lists of 10 top-ranked drugs, results of the proposed approach using 4 NSCLC datasets: GSE11969-adenocarcinoma, GSE11969-large cell carcinoma, GSE11969-squamous cell carcinoma, and GSE32863-adenocarcinoma. The scores for GSM1741743_sirolimus, GSM1738326_mocetinostat, and GSM1740080_sunitinib across NSCLC datasets are summarized in Table II. A score of 8 means that each candidate ranked higher than all 8 instances of FDA-approved drugs.

Figure 4: A systematic method to select repurposing drug candidates. A) Given a set of ranked lists of drugs (drug instances), we compute a score for each drug. B) We then calculate an average score for each drug instance across different lists (using disease datasets). C) Finally, we calculate an average score for each distinct drug across the instances, in case there are multiple instances for that drug.

3 Results

Table 2 shows the proposed candidates for treatment of four human diseases: IPF, NSCLC, prostate cancer, breast cancer, and preliminary evidences that support the usefulness of those candidates in treatment of the given diseases.

Table 2: *Preliminary support by preclinical or clinical studies showing the therapeutic potential of the proposed candidates. These candidates are currently FDA-approved but for other indications.*

Disease	Proposed candidate	Preclinical/clinical evidence	ClinicalTrials.gov ID
IPF	Sunitinib	[48, 122, 75]	
	Dabrafenib	[163, 104, 86]	
	Nilotinib	[6, 52, 4, 18, 1, 24, 120, 47]	
NSCLC	Sunitinib	[137, 101]	NCT00372775,NCT00092001,NCT00864721,NCT00693992
	Sirolimus	[14, 130, 46, 37]	NCT00923273
	Everolimus	[46, 138, 113]	NCT01061788
	Ponatinib	[22, 23, 118, 39, 147, 41]	NCT01813734
Prostate cancer	Podophyllotoxin	[44, 25, 74, 11, 29, 55, 84]	
	Acetylsalicylic acid	[100, 49, 62, 128, 28, 135, 85, 13]	NCT02757365,NCT03103152,NCT02804815
	Papaverine	[45, 132, 58]	
	Mefloquine	[42, 134, 158]	
	Vorinostat	[15, 34, 19, 69]	NCT00330161,NCT00589472
	Sirolimus	[20, 5, 116, 59]	NCT00311623,NCT02565901
Breast cancer	Captopril	[125, 65, 68, 76, 129, 98]	NCT00086723
	Glibenclimiade	[109, 2, 114, 161, 102, 124]	
	Fluorometholone	[71, 81, 66]	
	Etoposide	[8, 166, 165]	NCT01492556,NCT00026949,NCT01589159
	Colchicine	[141]	
	Tretinoin	[142, 17, 83, 108, 40]	

3.1 Idiopathic pulmonary fibrosis (IPF)

The list of IPF datasets we used in our analysis is summarized in Table 3.

Table 3: Idiopathic pulmonary fibrosis (IPF) datasets

Dataset	Source	Samples
GSE1724	NCBI GEO [119]	Treated (TGFbeta) vs untreated
GSE21369	NCBI GEO [27]	Interstitial lung disease vs healthy
GSE24206-advanced	NCBI GEO [94]	Advance stage IPF vs healthy
GSE24206-early	NCBI GEO [94]	Early stage IPF vs healthy
GSE44723	NCBI GEO [111]	Rapid progressing IPF vs healthy
LGRC	Lung Genomics Research Consortium	Interstitial lung disease vs healthy

Gold standard: Nintedanib is the only FDA-approved drug for IPF in our drug input datasets (highlighted as green). It inhibits *RTKs* such as *PDGFR* (α , β), *FGFR(1,2,3)*, *VEGFR(1,2,3)*, and *FLT*3, among them, *FGFR*, *PDGFR*, and *VEGFR* have been implicated in the pathogenesis of IPF. Additionally, Nintedanib inhibits *nRTKs* such as *Lck*, *Lyn* and *Src kinases* [70, 115, 92, 140, 51, 155, 47].

We select the top 5% of drugs ranked lists obtained by applying the proposed approach on 6 IPF datasets. As shown in Table 4, these drugs are ranked from the highest to the lowest, based on their scores. The score assigned to Nintedanib

Table 4: The top 5% drugs obtained from the result of our repurposing approach. These drugs are ranked based on the scores generated by the systematic method. The * denotes the drugs that are currently FDA-approved but for other indications. The score for Nintedanib, the FDA-approved drug for IPF, is 0. Drugs with the same scores are sorted based on their average ranks.

Drug	Score
Saracatinib	1.5
Nintedanib	0
Linifanib	-0.67
Sunitinib *	-1.42
Buparlisib	-1.83
GDC-0941	-1.92
Alvocidib	-2.58
Dabrafenib *	-2.67
Nilotinib *	-2.83
Gefitinib *	-2.92
Idelalisib *	-2.92
CH5424802	-3
Everolimus *	-3
Dovitinib	-3
Rucaparib *	-3.08
Celastrol	-3.08
NVP-BEZ235	-3.17
Selumetinib	-3.17
Erlotinib *	-3.58
Sirolimus *	-3.58

is 0. Since we have four instances for Nintedanib, drugs scores range between -4 and 4. The largest negative score for a drug indicates that drug ranked worse than all four instances of Nintedanib. Drugs with the same scores are sorted based on their average ranks in drugs ranked lists.

3.1.1 Drug-disease networks

We used chord diagrams to represent subnetworks of drug-disease networks (DDN) for Nintedanib (Figure 5), Sunitinib (Figure 6), Linifanib (Figure 7), and Saracatinib (Figure 8). In order to obtain the subnetworks we use IPF-associated genes belonging to the *Pathways in cancer*, the target pathway for Nintedanib. The subnetwork S= (V,E) with the node set V and edge set E is represented as follow:

$$S = (V, E) : (V \subset Path \cap (Disease_t \cup Drug_t)) \wedge (E \subset DDN) \tag{1}$$

where $Disease_t = \{x_1, x_2, ..., x_n\}$, $Drug_t = \{y_1, y_2, ..., y_n\}$, and $Path$ denote the disease-related genes, drug targets, and the genes on the *Pathways in cancer*, respectively.

In the chord diagram, sectors represent the genes and the chords represent the associations between various genes in the network we built. The red sectors represent the genes known to be associated to IPF. The green sectors represent the genes targeted by Nintedanib.

In addition to chord diagrams, we used the edge lists to represent the DDN subnetworks we construct for the repurposing candidates. In this list, the association between the genes is represented as a tuple (e.g. FGFR1 - KRAS). Table 5 shows the edge lists representing DDN subnetworks for repurposing drugs: Nintedanib, Nilotinib, and Sunitinib. Table 6 shows the edge lists representing DDN subnetworks for drugs: Linifanib and Saracatinib. These drugs are currently undergoing clinical trials for several indications (see detail in section 3.1 of the manuscript). Red entires represent genes known to be associated to IPF disease. Entries representing the Nintedanib target genes are green.

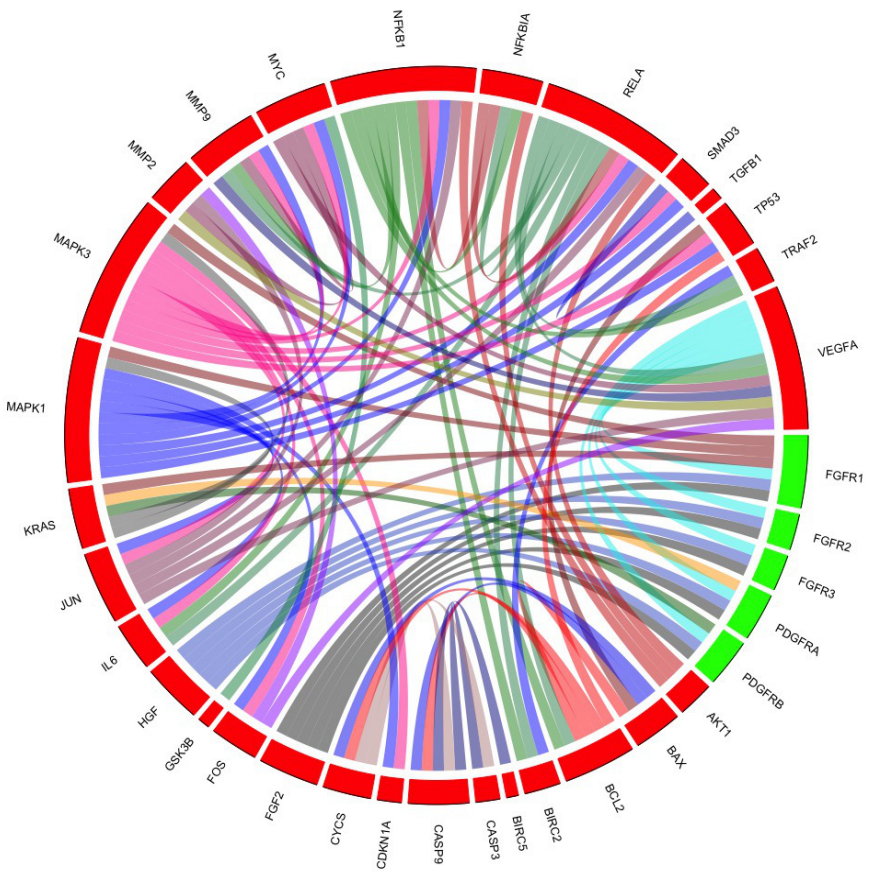

Figure 5: The chord diagram represents the subnetwork of DDN for Nintedanib, the FDA-approved drug for IPF. In order to obtain this subnetwork, we used IPF-associated genes that are included in KEGG's *Pathways in cancer* (the target pathway for Nintedanib). Sectors and chords represent the genes and associations between the genes in the network, respectively. Red sectors represent genes known to be associated to IPF disease. Sectors representing the Nintedanib target genes are green.

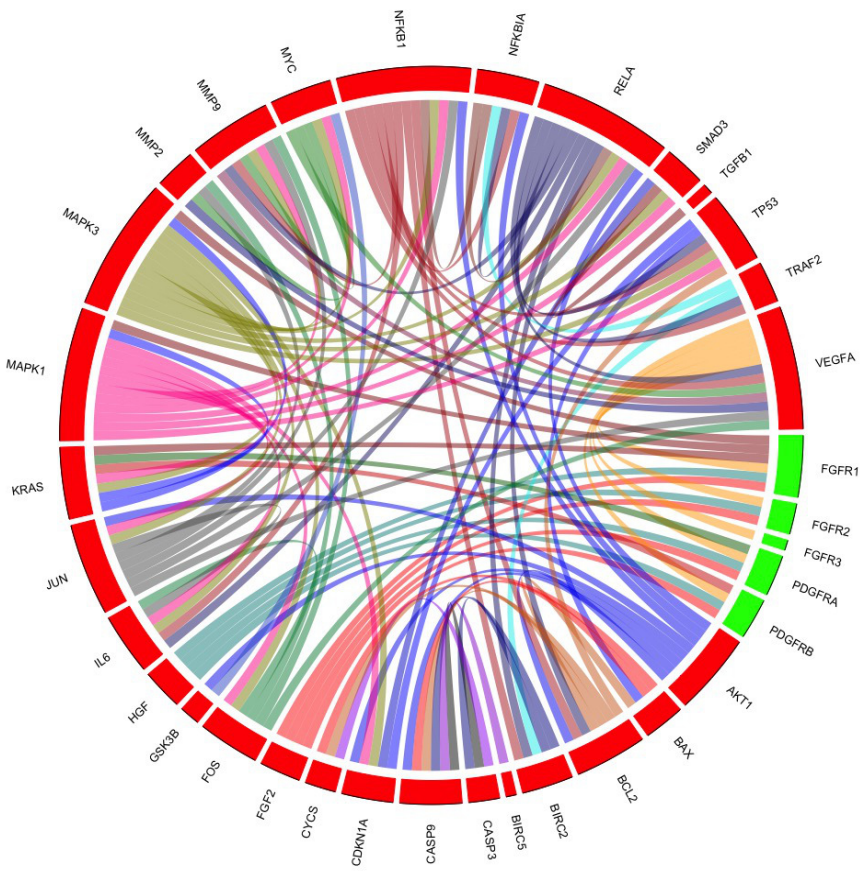

Figure 6: The chord diagram represents the subnetwork of DDN for Sunitinib, the repurposing candidate for the treatment of IPF. In order to obtain this subnetwork, we used IPF-associated genes that are included in KEGG's *Pathways in cancer* (the target pathway for Nintedanib). Sectors and chords represent the genes and associations between the genes in the network, respectively. Red sectors represent genes known to be associated to IPF disease. Sectors representing the Nintedanib target genes are green.

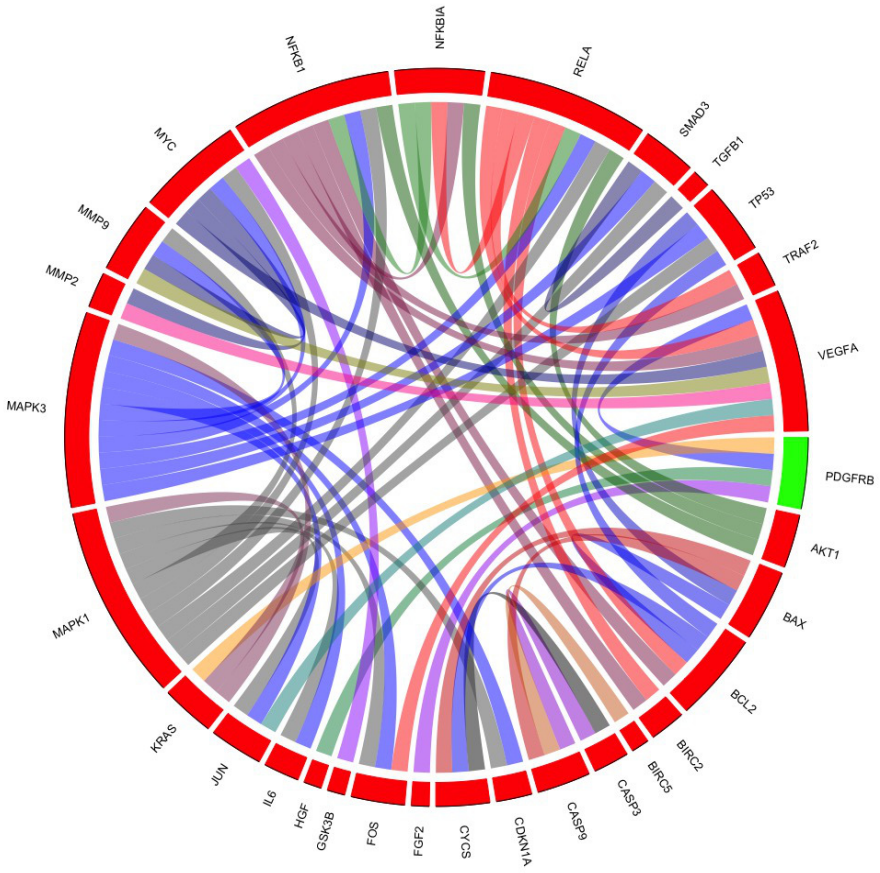

Figure 7: The chord diagram represents the subnetwork of DDN for Linifanib. In order to obtain this subnetwork, we used IPF-associated genes that are included in KEGG's *Pathways in cancer* (the target pathway for Nintedanib). Sectors and chords represent the genes and associations between the genes in the network, respectively. Red sectors represent genes known to be associated to IPF disease. Sectors representing the Nintedanib target genes are green.

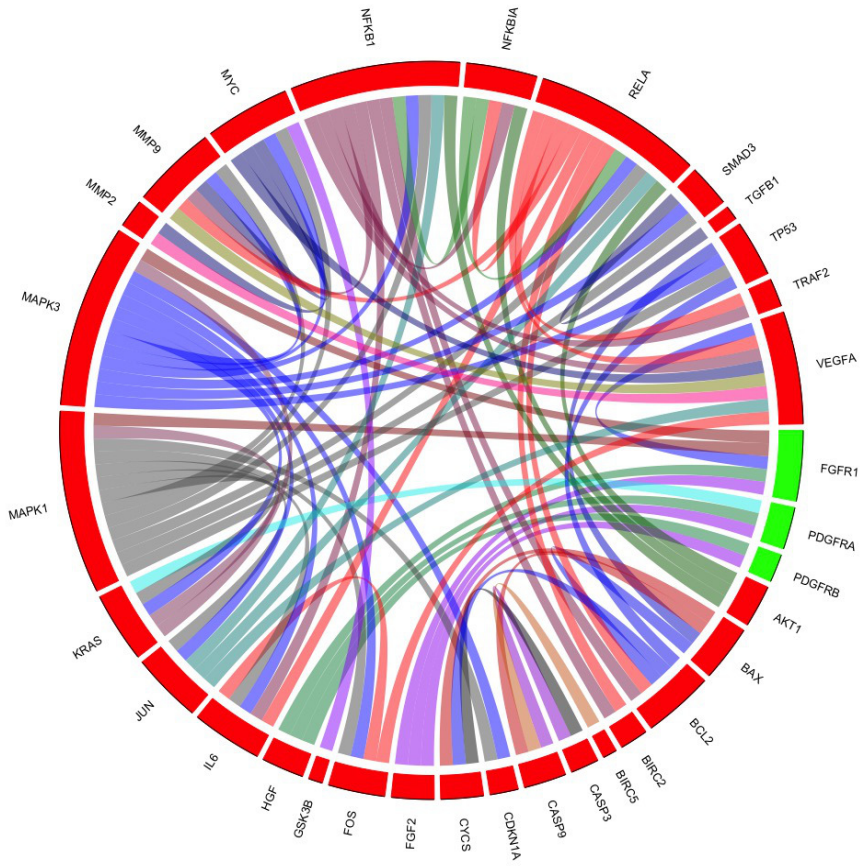

Figure 8: The chord diagram represents the subnetwork of DDN for Saracatinib. In order to obtain this subnetwork, we used IPF-associated genes that are included in KEGG's *Pathways in cancer* (the target pathway for Nintedanib). Sectors and chords represent the genes and associations between the genes in the network, respectively. Red sectors represent genes known to be associated to IPF disease. Sectors representing the Nintedanib target genes are green.

Table 5: The edge lists represent the subnetwork of DDN of drugs: Nintedanib, Nilotinib, and Sunitinib. Nintedanib is the FDA-approved drug for IPF treatment. Nilotinib and Sunitinib are the repurposing candidates for the treatment of IPF. In this list, the association between two genes is represented as gene pairs. In order to obtain the subnetworks, we used IPF-associated genes that are included in KEGG's *Pathways in cancer* (the target pathway for nintedanib). Red entires represent genes known to be associated to IPF disease. Entries representing the Nintedanib target genes are green.

Nintedanib			
Gene1 → Gene2		Gene1 → Gene2	
FGFR1	KRAS	JUN	VEGFA
FGFR1	MAPK1	KRAS	MAPK1
FGFR1	MAPK3	KRAS	MAPK3
PDGFRα	KRAS	MAPK1	CDKN1A
PDGFRβ	KRAS	MAPK1	IL6
FGF2	FGFR1	MAPK1	MMP9
FGF2	FGFR2	MAPK1	MYC
FGF2	FGFR3	MAPK1	NFKB1
FGF2	PDGFRα	MAPK1	RELA
FGF2	PDGFRβ	MAPK1	TP53
HGF	FGFR1	MAPK3	CDKN1A
HGF	FGFR2	MAPK3	IL6
HGF	FGFR3	MAPK3	MMP9
HGF	PDGFRα	MAPK3	MYC
HGF	PDGFRβ	MAPK3	NFKB1
VEGFA	FGFR1	MAPK3	RELA
VEGFA	FGFR2	MAPK3	TP53
VEGFA	FGFR3	MYC	MMP2
VEGFA	PDGFRα	MYC	MMP9
VEGFA	PDGFRβ	MYC	VEGFA
AKT1	NFKB1	NFKB1	BCL2
AKT1	NFKBIA	NFKB1	BIRC2
AKT1	RELA	NFKB1	IL6
BAX	CASP9	NFKB1	MMP9
BAX	CYCS	NFKB1	NFKBIA
BIRC5	CASP9	NFKB1	TRAF2
CASP9	CASP3	NFKB1	VEGFA
CYCS	CASP3	RELA	BCL2
CYCS	CASP9	RELA	BIRC2
FOS	MMP2	RELA	IL6
FOS	VEGFA	RELA	MMP9
JUN	MMP2	RELA	NFKBIA
JUN	NFKB1	RELA	TRAF2
JUN	RELA	RELA	VEGFA
JUN	VEGFA	TGFB1	SMAD3
KRAS	MAPK1	TRAF2	BIRC2

Nilotinib			
Gene1 → Gene2		Gene1 → Gene2	
PDGFRα	KRAS	MYC	VEGFA
PDGFRβ	KRAS	NFKB1	BCL2
FGF2	PDGFRα	NFKB1	BIRC2
FGF2	PDGFRβ	NFKB1	IL6
HGF	PDGFRα	NFKB1	MMP9
HGF	PDGFRβ	NFKB1	NFKBIA
VEGFA	PDGFRα	NFKB1	TRAF2
VEGFA	PDGFRβ	NFKB1	VEGFA
AKT1	NFKB1	RELA	BCL2
AKT1	NFKBIA	RELA	BIRC2
AKT1	RELA	RELA	IL6
BAX	CASP9	RELA	MMP9
BAX	CYCS	RELA	NFKBIA
BIRC5	CASP9	RELA	TRAF2
CASP9	CASP3	RELA	VEGFA
CYCS	CASP3	TGFB1	SMAD3
FOS	VEGFA		
JUN	VEGFA		
KRAS	MAPK1		
KRAS	MAPK3		
MAPK1	CDKN1A		
MAPK1	IL6		
MAPK1	MMP9		
MAPK1	MYC		
MAPK1	NFKB1		
MAPK1	RELA		
MAPK1	TP53		
MAPK3	CDKN1A		
MAPK3	IL6		
MAPK3	MMP9		
MAPK3	MYC		
MAPK3	NFKB1		
MAPK3	RELA		
MAPK3	TP53		
MYC	MMP2		
MYC	MMP9		

Sunitinib			
Gene1 → Gene2		Gene1 → Gene2	
FGFR1	KRAS	JUN	VEGFA
FGFR1	MAPK1	KRAS	MAPK1
FGFR1	MAPK3	KRAS	MAPK3
PDGFRα	KRAS	MAPK1	CDKN1A
PDGFRβ	KRAS	MAPK1	IL6
FGF2	PDGFRα	MAPK1	MMP9
FGF2	PDGFRβ	MAPK1	MYC
HGF	FGFR1	MAPK1	NFKB1
HGF	FGFR2	MAPK1	RELA
HGF	PDGFRα	MAPK1	TP53
HGF	PDGFRβ	MAPK3	CDKN1A
VEGFA	FGFR1	MAPK3	IL6
VEGFA	FGFR2	MAPK3	MMP9
VEGFA	FGFR3	MAPK3	MYC
VEGFA	PDGFRα	MAPK3	NFKB1
VEGFA	PDGFRβ	MAPK3	RELA
FGF2	FGFR1	MAPK3	TP53
FGF2	FGFR2	MYC	MMP2
AKT1	BCL2	MYC	MMP9
AKT1	NFKB1	MYC	VEGFA
AKT1	NFKBIA	NFKB1	BCL2
AKT1	RELA	NFKB1	BIRC2
BAX	CASP9	NFKB1	IL6
BAX	CYCS	NFKB1	MMP9
BIRC5	CASP9	NFKB1	NFKBIA
CASP9	CASP3	NFKB1	TRAF2
CYCS	CASP3	NFKB1	VEGFA
FOS	IL6	RELA	BCL2
FOS	MMP2	RELA	BIRC2
FOS	MMP9	RELA	IL6
FOS	VEGFA	RELA	MMP9
JUN	IL6	RELA	NFKBIA
JUN	MMP2	RELA	TRAF2
JUN	MMP9	RELA	VEGFA
JUN	NFKB1	SMAD3	CDKN1A
JUN	RELA	TGFB1	SMAD3
		TP53	CDKN1A
		TRAF2	BIRC2
		TRAF2	NFKBIA

Table 6: The edge lists represent the subnetwork of DDN of drugs: linifanib and saracatinib. These drugs are currently undergoing clinical trials (for conditions other than IPF) that can be considered for the treatment of IPF. In this list, the association between two genes is represented as a tuple. In order to obtain the subnetworks, we used IPF-associated genes that are included in KEGG's *Pathways in cancer* (the target pathway for nintedanib). Red entires represent genes known to be associated to IPF disease. Entries representing the Nintedanib target genes are green.

Linifanib	
Gene1 →	Gene2
PDGFRβ	KRAS
FGF2	PDGFRβ
HGF	PDGFRβ
VEGFA	PDGFRβ
AKT1	NFKB1
AKT1	NFKBIA
AKT1	RELA
BAX	CASP9
BAX	CYCS
BIRC5	CASP9
CASP9	CASP3
CYCS	CASP3
JUN	VEGFA
KRAS	MAPK1
KRAS	MAPK3
MAPK1	CDKN1A
MAPK1	IL6
MAPK1	MMP9
MAPK1	MYC
MAPK1	NFKB1
MAPK1	RELA
MAPK1	TP53
MAPK3	CDKN1A
MAPK3	IL6
MAPK3	MMP9
MAPK3	MYC
MAPK3	NFKB1
MAPK3	RELA
MAPK3	TP53
MYC	MMP2
MYC	MMP9
MYC	VEGFA
NFKB1	BCL2
NFKB1	BIRC2
NFKB1	NFKBIA
NFKB1	TRAF2
NFKB1	VEGFA
RELA	BCL2
RELA	BIRC2
RELA	NFKBIA
RELA	TRAF2
RELA	VEGFA
TGFB1	SMAD3

Saracatinib			
Gene1 →	Gene2	Gene1 →	Gene2
FGFR1	MAPK1	NFKB1	BIRC2
FGFR1	MAPK3	NFKB1	IL6
PDGFRα	KRAS	NFKB1	MMP9
FGF2	PDGFRα	NFKB1	NFKBIA
FGF2	PDGFRβ	NFKB1	TRAF2
HGF	PDGFRα	NFKB1	VEGFA
HGF	PDGFRβ	RELA	BCL2
VEGFA	FGFR1	RELA	BIRC2
AKT1	NFKB1	RELA	IL6
AKT1	NFKBIA	RELA	MMP9
AKT1	RELA	RELA	NFKBIA
BAX	CASP9	RELA	TRAF2
BAX	CYCS	RELA	VEGFA
BIRC5	CASP9	TGFB1	SMAD3
CASP9	CASP3		
CYCS	CASP3		
FGF2	FGFR1		
FOS	IL6		
FOS	VEGFA		
HGF	FGFR1		
JUN	NFKB1		
JUN	RELA		
JUN	VEGFA		
KRAS	MAPK1		
KRAS	MAPK3		
MAPK1	CDKN1A		
MAPK1	IL6		
MAPK1	MMP9		
MAPK1	MYC		
MAPK1	NFKB1		
MAPK1	RELA		
MAPK1	TP53		
MAPK3	CDKN1A		
MAPK3	IL6		
MAPK3	MMP9		
MAPK3	MYC		
MAPK3	RELA		
MAPK3	TP53		
MYC	MMP2		
MYC	MMP9		
MYC	VEGFA		
NFKB1	BCL2		
NFKB1	BIRC2		

3.1.2 Drug-drug networks

Figures 9 and 10 show the drug-drug networks we generated using the known knowledge (target pathways and target genes) of Nintedanib (FDA-approved for IPF treatment) and top-ranked candidates for IPF, where circles correspond to drugs, and two drugs being connected if they share target pathways or target genes, respectively. The target pathways and target genes of drugs (represented by rectangles) are obtained from KEGG and Drugbank [154].

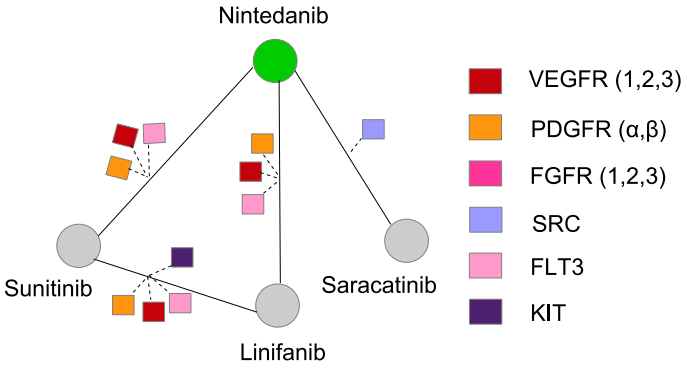

Figure 9: Drug-drug network is generated using the known knowledge of drugs target genes, obtained from KEGG and Drugbank [154]. Circles and rectangles correspond to drugs and target genes, respectively. Drugs are connected to each other based on their common target genes. Nintedanib (shown with green circle) is FDA-approved for treatment of IPF. *VEGFR(1,2,3)*, *PDGFR* (α,β), *FGFR (1,2,3)*, *SRC*, *FLT3*, and *KIT* are known to be target genes of Nintedanib [70, 115, 92, 140, 51, 155, 47].

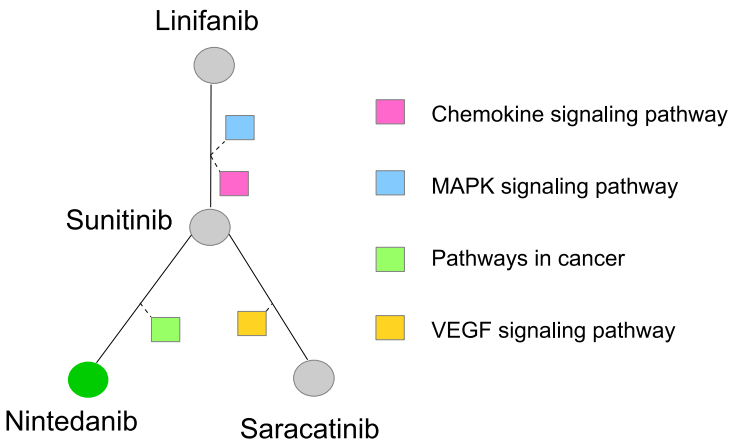

Figure 10: Drug-drug network is generated using the known knowledge of drugs target pathways, obtained from KEGG. Circles and rectangles correspond to drugs and target pathways, respectively. Drugs are connected to each other based on their common target pathways. Nintedanib (shown with green circle) is FDA-approved for treatment of IPF. *Pathways in cancer* is known as the target pathway for Nintedanib.

3.2 Non-small cell lung cancer

We obtained four non-small cell lung cancer (NSCLC) datasets from Gene Expression Omnibus (GEO): GSE32863 (adenocarcinoma) [133] and GSE11969 (subtypes: adenocarcinoma, large cell carcinoma, squamous cell carcinoma) [144]. Adenocarcinoma (40% of lung cancers), squamous cell carcinoma (25% of lung cancers), and large cell carcinoma (10% of lung cancers) are three main subtypes of NSCLC.

Gold standards: Gefitinib and Crizotinib are the FDA-approved drugs for treatment of NSCLC. These drugs are included in our list of input drugs from LINCS. On all NSCLC datasets, three computational approaches were compared in terms of their ability to highly rank the instances of Gefitinib and Crizotinib that exist in the LINCS drug database.

Erlotinib is used as the maintenance treatment of locally advanced or metastatic NSCLC patients with no progress in their disease after four cycles of platinum-based first-line chemotherapy. It is also indicated after failure of at least one prior chemotherapy regimen in patients with NSCLC. Since Erlotinib is limited to very specific patients with NSCLC and none of our datasets fulfill such limitations, we did not consider it as the gold standard. However, the proposed approach is significantly better than the other two approaches even if Erlotinib were to be included as the gold standard.

Tables 8–11 show the results obtained on four NSCLC datasets using: i) the proposed approach, ii) the drug-disease approach, and iii) the anti-correlation approach. The FDA-approved drugs for NSCLC are highlighted in green.

We selected the top 5% of drugs ranked lists obtained by applying the proposed approach using 4 NSCLC datasets. As shown in Table 7, these drugs are ranked according to the scores computed by the systematic method from the highest to the lowest. The sum of the scores assigned to Gefitinib and Crizotinib (the FDA-approved drugs for NSCLC) is 0. Drugs with the same scores are sorted based on their average ranks in drugs ranked lists.

Proposed candidates: We propose the FDA-approved drugs: Sunitinib ($p = 0.0009$), Sirolimus ($p = 0.0009$), Enzastaurin ($p = 0.0009$), Everolimus ($p = 0.001$), and Ponatinib ($p = 0.004$) as repurposing candidates for treatment of NSCLC. Although Mocetinostat, Roscovitine, and Saracatinib are not approved by FDA yet, they can be prioritized for further investigations.

As discussed earlier, **Sunitinib** is an oral, small-molecule that inhibits RTKs, including VEGFR and PDGFR. Recent clinical trials have reported that Sunitinib has the provocative single-agent activity in previously treated patients with recurrent and advanced NSCLC [137, 101]. Sunitinib has completed the phase II of clinical trials for treatment of patients with NSCLC (ClinicalTrials.gov IDs: NCT00372775, NCT00092001, NCT00864721). The phase III of clinical trials on Sunitinib as a potential maintenance therapy in NSCLC patients has been completed. These patients had received four cycles of platinum-based chemotherapy

Table 7: The top 5% of drugs obtained from the result of the proposed approach. These drugs are ranked based on the scores generated by the systematic method. The * denotes the drugs that are currently FDA-approved but for other indications. Gefitinib and Crizotinib, as highlighted with green, are FDA-approved for the treatment of NSCLC. Drugs with the same scores are sorted based on their average ranks in drugs ranked lists.

Drug	Score
Sunitinib *	4.625
Mocetinostat	2.75
Gefitinib	1.75
Roscovitine	-1
Sirolimus *	-1
Enzastaurin *	-1.75
Crizotinib	-1.75
Everolimus *	-2
Ponatinib *	-2.25
Saracatinib	-2.25
Rucaparib *	-3.125
Dasatinib *	-3.375
Linifanib	-3.625
Mitoxantrone *	-4.625

without disease progression. The result of the trials has not published yet (ClinicalTrials.gov ID: NCT00693992).

Sirolimus, also known as Rapamycin, is a potent immunosuppressant that inhibits mammalian target of rapamycin (mTOR). The positive effect of Sirolimus in inhibiting the growth and progression of NSCLC is supported by several clinical studies [37, 14, 130, 46]. The phase I/II clinical trials have been launched to test the efficiency of Sirolimus in combination with Pemetrexed for treating patients with NSCLC (ClinicalTrials.gov ID: NCT01061788). The phase I clinical trials of Sunitinib and Sirolimus confirm that this combination is well-tolerated and warrants further investigation in advanced NSCLC [152](ClinicalTrials.gov ID: NCT00555256).

Everolimus is a derivative of rapamycin (Sirolimus). It is approved by FDA for treatment of several conditions, including breast cancer, advanced renal cell carcinoma, renal angiomyolipoma, and tuberous sclerosis. It has shown antitumor activity both as the single agent and in combination with other agents in treatment of patients with NSCLC. Several clinical trials support the efficacy of Everolimus in treatment of NSCLC [113, 138, 46, 148] (ClinicalTrials.gov ID: NCT00096486).

Increased levels of protein kinase C (PKC) and AKT are known to be associated with the poor prognosis in NSCLC [32, 103]. **Enzastaurin**, an oral serine/threonine kinase inhibitor, suppresses PKC and protein kinase B/AK transforming (AKT) signaling, induces tumor cell apoptosis, and inhibits the proliferation and angiogenesis [103]. Enzastaurin is proven to inhibit the growth of NSCLC cell lines [97, 146, 103]. The Phase II evaluation of Enzastaurin as

the second-and third- line treatment for NSCLC has completed with promising results (ClinicalTrials.gov ID: NCT00105092).

Fibroblast growth factor receptors (FGFRs) are known to be overexpressed in NSCLC [131, 10]. **Ponatinib** is proven to be effective against the FGFR1 kinase in 8p11 myeloproliferative syndrome (EMS) [23]. In particular, It has been shown that Ponatinib can suppress cell growth in NSCLC cell lines [118, 147]. Several studies reported that RET fusions are viable targets in NSCLC [41, 39, 22]. The phase II of the clinical trial (ClinicalTrials.gov ID: NCT01813734) is currently evaluating the safety and the effectiveness of the RET inhibitor Ponatinib in treating patients with NSCLC.

It has been reported that HDAC inhibitor **Mocetinostat** may restore normal cell function and reduce or inhibit the tumor growth [99]. A phase 1/2 clinical trial of Mocetinostat, in combination with Durvalumab is currently ongoing in treating patients with solid tumors and NSCLC to evaluate the safety and efficacy of this combination [50] (ClinicalTrials.gov IDs: NCT02805660). Another clinical trial is currently undergoing to evaluate the clinical activity of Nivolumab in combination with three separate drugs, Glesatinib, Sitravatinib, or Mocetinostat in NSCLC (ClinicalTrials.gov ID: NCT02954991, phase II).

Roscovitine is an experimental drug in the class of pharmacological cyclin-dependent kinase (CDK) inhibitors. Current clinical studies [105, 31] suggest the combination of Roscovitine and Belinostat in treating patients with NSCLC. The phase II study of Roscovitine as a single agent in previously-treated patients with non-small cell lung cancer has terminated with no data reported (ClinicalTrials.gov ID: NCT00372073).

Saracatinib is an inhibitor of SRC kinases that may improve NSCLC treatment [126, 127, 167]. It is undergoing phase II of clinical trials in treatment of patients with NSCLC. (ClinicalTrials.gov ID: NCT00638937).

Table 8: A comparison between the results of three approaches: proposed, drug-disease, anti-correlation using GSE11969-adenocarcinoma dataset (the top 10 drugs). The p-values for Wilcoxon rank sum test comparing the results of the proposed approach with drug-disease and anti-correlation approaches are 0.01 and 0.005, respectively. Drugs highlighted with green are FDA-approved for the treatment of NSCLC. The * denotes the drugs that are currently FDA-approved but for other indications.

GSE11969-adenocarcinoma Proposed	Drug-disease	Anti-correlation
GSM1741743_sirolimus*	GSM1746780_erlotinib*	GSM1737411_NVP-BGT226
GSM1741104_sunitinib*	GSM1738326_mocetinostat	GSM1739358_mocetinostat
GSM1738326_mocetinostat	GSM1739358_mocetinostat	GSM1741104_sunitinib*
GSM1739358_mocetinostat	GSM1741104_sunitinib*	GSM1740576_BI-2536
GSM1746613_enzastaurin	GSM1745191_NVP-BEZ235	GSM1738326_mocetinostat
GSM1742552_linifanib	GSM1745674_dovitinib	GSM1740923_BI-2536
GSM1742645_gefitinib	GSM1742797_palbociclib*	GSM1737409_NVP-BGT226
GSM1740080_sunitinib*	GSM1745194_NVP-BEZ235	GSM1742797_palbociclib*
GSM1737700_rucaparib*	GSM1746864_radicicol	GSM1737349_everolimus*
GSM1744393_gefitinib	GSM1741767_vorinostat*	GSM1745194_NVP-BEZ235

Table 9: A comparison between the results of three approaches: proposed, drug-disease, anti-correlation using GSE11969-large cell carcinoma dataset (the top 10 drugs). The p-values for Wilcoxon rank sum test comparing the results of the proposed approach with drug-disease and anti-correlation approaches are 0.001 and 0.0005, respectively. Drugs highlighted with green are FDA-approved for the treatment of NSCLC. The * denotes the drugs that are currently FDA-approved but for other indications.

GSE11969-large cell carcinoma Proposed	Drug-disease	Anti-correlation
GSM1741743_sirolimus*	GSM1745191_NVP-BEZ235	GSM1737411_NVP-BGT226
GSM1741104_sunitinib*	GSM1738326_mocetinostat	GSM1740576_BI-2536
GSM1739358_mocetinostat	GSM1739358_mocetinostat	GSM1740923_BI-2536
GSM1738326_mocetinostat	GSM1745194_NVP-BEZ235	GSM1745191_NVP-BEZ235
GSM1740080_sunitinib*	GSM1745149_GDC-0980	GSM1745194_NVP-BEZ235
GSM1741800_mitoxantrone*	GSM1741767_vorinostat*	GSM1739358_mocetinostat
GSM1744393_gefitinib	GSM1737642_mocetinostat	GSM1745149_GDC-0980
GSM1742645_gefitinib	GSM1738308_entinostat	GSM1737409_NVP-BGT226
GSM1746613_enzastaurin	GSM1742797_palbociclib*	GSM1737410_NVP-BGT226
GSM1742878_dasatinib*	GSM1739435_belinostat*	GSM1741767_vorinostat*

Table 10: A comparison between the results of three approaches: proposed, drug-disease, anti-correlation using GSE11969-large cell carcinoma dataset (the top 10 drugs). The p-values for Wilcoxon rank sum test comparing the results of the proposed approach with drug-disease and anti-correlation approaches are 0.001 and 0.0003, respectively. Drugs highlighted with green are FDA-approved for the treatment of NSCLC. The * denotes the drugs that are currently FDA-approved but for other indications.

GSE11969-squamous cell carcinoma		
Proposed	Drug-disease	Anti-correlation
GSM1741743_sirolimus*	GSM1739358_mocetinostat	GSM1737411_NVP-BGT226
GSM1741104_sunitinib*	GSM1738326_mocetinostat	GSM1740576_BI-2536
GSM1740080_sunitinib*	GSM1746780_erlotinib*	GSM1745149_GDC-0980
GSM1738326_mocetinostat	GSM1742797_palbociclib*	GSM1745194_NVP-BEZ235
GSM1746613_enzastaurin	GSM1737642_mocetinostat	GSM1739358_mocetinostat
GSM1739358_mocetinostat	GSM1742706_alvocidib	GSM1741767_vorinostat*
GSM1744393_gefitinib	GSM1745912_neratinib*	GSM1737410_NVP-BGT226
GSM1742878_dasatinib*	GSM1737967_entinostat	GSM1737409_NVP-BGT226
GSM1740081_sunitinib*	GSM1738308_entinostat	GSM1745191_NVP-BEZ235
GSM1740917_saracatinib	GSM1737624_entinostat	GSM1741769_sirolimus*

Table 11: A comparison between the results of three approaches: proposed, drug-disease, anti-correlation using GSE32863 dataset (the top 10 drugs). The p-values for Wilcoxon rank sum test comparing the results of the proposed approach with drug-disease and anti-correlation approaches are 0.007 and 0.007, respectively. Drugs highlighted with green are FDA-approved for the treatment of NSCLC. The * denotes the drugs that are currently FDA-approved but for other indications.

GSE32863-adenocarcinoma		
Proposed	Drug-disease	Anti-correlation
GSM1741743_sirolimus*	GSM1738326_mocetinostat	GSM1738326_mocetinostat
GSM1738326_mocetinostat	GSM1739358_mocetinostat	GSM1739453_decitabine*
GSM1741104_sunitinib*	GSM1743209_nintedanib*	GSM1746780_erlotinib*
GSM1740080_sunitinib*	GSM1746780_erlotinib*	GSM1739358_mocetinostat
GSM1739358_mocetinostat	GSM1746881_mitoxantrone*	GSM1742878_dasatinib*
GSM1742878_dasatinib*	GSM1746893_radicicol	GSM1743210_nintedanib*
GSM1744393_gefitinib	GSM1742797_palbociclib*	GSM1742797_palbociclib*
GSM1740301_ponatinib*	GSM1740576_BI-2536	GSM1742706_alvocidib
GSM1740081_sunitinib*	GSM1740298_ponatinib*	GSM1744393_gefitinib
GSM1742552_linifanib	GSM1741767_vorinostat*	GSM1740576_BI-2536

3.3 Prostate cancer

We use three different prostate cancer datasets. The first dataset is obtained by comparing gene expression levels between prostate tissues from 6 prostate cancer samples with 6 healthy samples using Affymetrix Human Genome U133 Plus2.0 Array. This dataset is available via GEO (GSE26910) [112]. GSE6919 is the second dataset that compares 65 primary prostate cancer samples with 18 healthy samples using Affymetrix Human Genome U95A Version 2 Array [164, 21]. The third dataset is the result of comparing gene expression levels between 69 prostate cancer patients and 18 normal patients using Affymetrix Human Genome U133A 2.0 Array. This dataset is available in GEO (GSE6956) [150].

Gold standard: Nilutamide is the FDA-approved drug for the treatment of prostate cancer. This antiandrogen drug is included in our list of input drugs from Connectivity Map. Prostate cancer mostly depends on the androgen for the growth and survival. Nilutamide is known to block the action of androgens of adrenal and testicular origin that stimulate the growth of the normal and malignant prostatic tissue [67].

Tables 13–15 show the results obtained on 3 prostate cancer datasets using: i) the proposed approach, ii) the drug-disease approach, and iii) the anti-correlation approach.

We selected the top 5% drugs from the drugs ranked lists obtained by applying the proposed approach on 3 prostate cancer datasets. As shown in Table 12, these drugs are ranked according to the scores computed by the systematic method from the highest to the lowest. The score assigned to Nilutamide is 0. Drugs with the same scores are sorted based on their average ranks in drugs ranked lists.

Proposed candidates: In this case study, we chose Podophyllotoxin ($p = 0.2$), Acetylsalicylic acid ($p = 0.2$), Papaverine ($p = 0.01$), Mefloquine ($p = 0.03$), Vorinostat ($p = 0.1$), and Sirolimus ($p = 0.06$) for further evaluations.

Podophyllotoxin is a natural product found in podophyllin resin from the roots of podophyllum plants. Podophyllotoxin and its derivatives, including Deoxypodophyllotoxin, are reported to have significant anti-tumor effects in a number of cancers [84, 11, 29, 25, 74, 44]. A recent study demonstrated that Deoxypodophyllotoxin inhibits the cell proliferation and induces the cell apoptosis in human prostate cancer cells through the Akt/p53/Bax/PTEN signaling pathway, suggesting that Deoxypodophyllotoxin could be used as a novel chemotherapeutic drug for human prostate cancer [55].

Acetylsalicylic acid (Aspirin) is a nonsteroidal anti-inflammatory drug that is used for the temporary relief of different forms of pain, and the inflammation associated with various conditions. It is also indicated to decrease the risk of death and myocardial infarction in patients with chronic coronary artery disease. Recent findings confirm that the long duration regular Aspirin use modestly reduces the risk of prostate cancer [85, 135, 128, 49, 100, 62, 28]. Aspirin is also reported to affect the proliferation, apoptosis, resistance and metastasis

Table 12: The top 5% drugs obtained from the result of our repurposing approach. These drugs are ranked based on the scores generated by the systematic method. The * denotes the drugs that are currently FDA-approved but for other indications. The score for Nilutamide, the FDA-approved drug for prostate cancer, is 0. Drugs with the same scores are sorted based on their average ranks in drugs ranked lists.

Drug	Score
Podophyllotoxin *	0.33
Nilutamide	0
Acetylsalicylic acid *	-0.33
Papaverine *	-0.33
Mefloquine *	-0.33
Vorinostat *	-0.33
Sirolimus *	-0.33
Alprostadil *	-0.33
Glibenclamide *	-0.33
Oxyphenbutazone (discontinued/withdrawn)	-0.33
Phenelzine *	-0.33
Methylergometrine *	-0.33
Parthenolide	-0.33
Primaquine *	-0.33
Phenoxybenzamine *	-0.67
Etoposide *	-0.67
Captopril *	-0.67
Trichostatin A	-0.67
Fluorometholone *	-1

of prostate cancer cell lines, suggesting the further evaluation of the signaling cascades activated by Aspirin in order to improve diagnosis, prognosis and treatment of prostate cancer [13]. According to these findings, Aspirin can be used for both prevention and treatment purposes in prostate cancer (ClinicalTrials.gov IDs: NCT02757365, NCT03103152, NCT02804815).

Papaverine is a nonxanthine phosphodiesterase inhibitor that is indicated for the relief of the cerebral and peripheral ischemia. It induces morphologic differentiation and suppresses the proliferation of human prostate cancer cell [45]. Papaverine is reported to have antitumor effects in prostate cancer by inducing significant, highly selective and dose-dependent cytotoxic effects in cancer cells [58, 132].

Mefloquine (MQ) is a prophylactic anti-malarial drug which acts as a blood schizonticide and can be a potential treatment for prostate cancer. Recent findings indicate that MQ has anticancer effects in PC3, which is the most commonly used prostate cancer cell line [158, 159]. MQ has been reported to be potent in killing cancer cells in vitro, suggested as the chemotherapeutic agent for treatment of glioblastoma and breast cancer cells [42, 134].

Vorinostat is a histone deacetylase (HDAC) inhibitor approved by FDA for the treatment of patients with cutaneous T-cell lymphoma (CTCL). Inhibition of the HDAC has resulted in decreasing the tumor growth and reducing cell

Table 13: A comparison between the results of three approaches: proposed, drug-disease, anti-correlation using GSE26910 dataset (the top 10 drugs). The ranks of Nilutamide, the FDA-approved drug for prostate cancer, in the proposed approach, drug-disease and anti-correlation approaches results are 9, 13, and 63 , respectively. Drug highlighted with green is FDA-approved for the treatment of prostate cancer. The * denotes the drugs that are currently FDA-approved but for other indications.

GSE26910 Proposed	Drug-disease	Anti-correlation
mefloquine_5724 *	luteolin_3041	vorinostat_6179 *
mefloquine_2210 *	etoposide_1626 *	parthenolide_5530
podophyllotoxin_2540	vorinostat_6939 *	parthenolide_2885
vorinostat_6179 *	phenoxybenzamine_5248 *	tanespimycin_2666
phenoxybenzamine_5613 *	puromycin_3310	phenoxybenzamine_5248 *
oxyphenbutazone_6844	ciclopirox_2456 *	phenoxybenzamine_5613 *
parthenolide_2885	vorinostat_6179 *	doxazosin_3024 *
parthenolide_5530	anisomycin_1304 *	mycophenolic acid_2857 *
nilutamide_5362	lycorine_3808	etoposide_3241 *

proliferation in prostate cancer, suggesting that Vorinostat could be a potential drug for treatment of prostate cancer [69, 15, 19, 34] (ClinicalTrials.gov IDs: NCT00330161, NCT00589472).

The initial preclinical and clinical studies show that the mTOR inhibition **Sirolimus** can be useful in treating patients with prostate cancer [30, 59, 116, 20, 5]. Sirolimus and its combination with other drugs are undergoing clinical trials in treatment of patients with prostate caner (ClinicalTrials.gov IDs: NCT00311623, NCT02565901).

Table 14: A comparison between the results of three approaches: proposed, drug-disease, anti-correlation using GSE6919 dataset (the top 10 drugs). The ranks of Nilutamide, the FDA-approved drug for prostate cancer, in the proposed approach, drug-disease and anti-correlation approaches results are 7, 81, and 129, respectively. Drugs highlighted with green are FDA-approved for the treatment of prostate cancer. The * denotes the drugs that are currently FDA-approved but for other indications.

GSE6919 Proposed	Drug-disease	Anti-correlation
papaverine_1755 *	alvespimycin_1638	doxorubicin_3291 *
vorinostat_6179 *	daunorubicin_4983 *	doxorubicin_5671 *
etoposide_3241 *	tanespimycin_986	daunorubicin_4983 *
alprostadil_2938 *	doxorubicin_5671 *	mitoxantrone_3232 *
podophyllotoxin_2540*	alvespimycin_993	rifabutin_3873 *
methylergometrine_1607	mitoxantrone_3232 *	alvespimycin_1638
nilutamide_5362	etoposide_3241 *	alvespimycin_993
fluorometholone_6247 *	parthenolide_5530	oxyphenbutazone_6844
colchicine_1598 *	ciclopirox_3317 *	mitoxantrone_5354 *
acetylsalicylic acid_1042 *	mitoxantrone_5354 *	vorinostat_6939 *

Table 15: A comparison between the results of three approaches: proposed, drug-disease, anti-correlation using GSE6956 dataset (the top 10 drugs). The ranks of Nilutamide, the FDA-approved drug for prostate cancer in the proposed approach, drug-disease and anti-correlation approaches results are 15, 141, and 90, respectively. The * denotes the drugs that are currently FDA-approved but for other indications.

GSE6956 Proposed	Drug-disease	Anti-correlation
acetylsalicylic acid_1042 *	phenelzine_4360 *	phenelzine_4360 *
captopril_1988 *	rifabutin_4349 *	rifabutin_4349 *
sirolimus_1080 *	trichostatin A_5017	primaquine_4845 *
glibenclamide_1546 *	captopril_1988 *	norfloxacin_7283 *
phenelzine_4360 *	ambroxol_6719 *	flunixin_2552
sirolimus_987 *	metaraminol_2298 *	captopril_1988 *
trichostatin A_5017	sirolimus_1080 *	sirolimus_987 *
primaquine_4845 *	picrotoxinin_2161 *	trichostatin A_5017
paclitaxel_6720	cyproheptadine_6740 *	calmidazolium_906
ajmaline_1749 *	primaquine_4845 *	ambroxol_6719 *

3.4 Breast cancer

We obtained six breast cancer datasets, GSE1299 [93] and GSE28645 [151], and GSE65194 (subtypes: Her2, luminalA, luminalB, triple negative) [89, 88, 91] from Gene Expression Omnibus (GEO). Datasets GSE1299 and GSE65194 (Her2, luminalA, luminalB, triple negative) consist of two groups of samples such as disease and control, while the dataset GSE28645 is a gene expression dataset that consists of two groups of samples: treated (by tamoxifen) and untreated. It is well-known that choices of the treatment and the ultimate success for breast cancer highly depend on its specific type [43], that is categorized as:

- Hormone receptor positive (estrogen and/or progesterone receptor positive) or hormone receptor negative (estrogen and/or progesterone receptor negative)
- Human epidermal growth factor receptor (HER2/neu) positive or HER2/neu negative
- Triple negative (all estrogen receptor, progesterone receptor, and HER2/neu are negative)

Other factors that affect the prognosis and treatment options include: stage of the cancer, levels of estrogen receptor, progesterone receptor, or HER2/neu in the tumor tissue, the growth rate of the tumor, the recurrence rate, patient's age, and menopausal status.

Gold standard: Fulvestrant, Paclitaxel, Methotrexate are FDA-approved drugs for the treatment of breast cancer. These drugs are included in our list of input drugs from Connectivity Map. Table 16 represents the target genes and activity of these drugs, obtained from KEGG and Drugbank [154]. Tables 18–23 show the results obtained on 6 breast cancer datasets using: i) the proposed approach, ii) the drug-disease approach, and iii) the anti-correlation approach.

We selected the top 5% drugs from the drugs ranked lists obtained by applying the proposed approach on 6 breast cancer datasets. These drugs are ranked according to the scores computed by the systematic method from the highest to the lowest. Table 17 shows the rank-ordered list of such drugs according to their score.

Proposed candidates: For this disease, we propose Captopril ($p = 0.001$), Glibenclimiade ($p = 0.0009$), Fluorometholone ($p = 0.005$), Etoposide ($p = 0.01$), Colchicine ($p = 0.001$), and Tretinoin ($p = 0.0009$) as repurposing candidates for treatment of breast cancer.

Captopril is indicated for treatment of hypertension, congestive heart failure, and kidney problems caused by diabetes. Recent clinical studies confirm the potential antineoplastic effect of Captopril in cancer [129, 76, 68, 125, 65]. The phase I/II clinical trial (ClinicalTrials.gov ID: NCT00086723) evaluates the activity of Captopril and the tissue plasminogen activator (a blood factor/protein

orchestrating the breakdown of blood clot) in treating patients with progressive metastatic cancer. Specifically, Captopril is proven to play a role in prevention and regression of the tamoxifen-induced resistance of breast cancer cell line MCF-7 [98], suggesting that it can be used in combination with Tamoxifen to overcome such resistance.

Glibenclimiade is an antidiabetic drug that is used as an adjunct to diet and exercise for treatment of patients with type 2 diabete. Glibenclamide is proven to be a tumor growth inhibitor [124, 161, 114, 2, 109]. It is considered as a promising antitumor drug in several cancers, including breast cancer. In particular, the cytostatic effect of Glibenclimiade by inducing G0/G1 arrest has been clearly demonstrated in MDA-MB-231 cells. Additionally, the study of its effect in combination with Doxorubicin suggests the novel role of Glibenclimiade as an adjuvant in breast cancer treatment [102].

Fluorometholone and Clobetasol are in the family of glucocorticoids (GCs). GCs have shown some modest benefits in treatment of breast cancer. However, their underlying mechanism in breast cancer is not well-understood [81, 71, 66]. GCs are also used as an adjuvant during chemotherapy or radiotherapy to reduce the side effects in cancer treatment [156].

Etoposide is approved by FDA for the treatment of refractory testicular tumors, and usually used in combination with other chemotherapeutic agents. It is also used as the first line treatment in small cell lung cancer patients. The positive therapeutic effect of Etoposide in patients with breast cancer is experimentally validated by clinical studies [8, 166] (ClinicalTrials.gov identifiers: NCT01492556, NCT00026949, and NCT01589159).

The histone deacetylase (HDAC) inhibitor Trichostatin A (TSA) is another drug we suggest for treatment of breast cancer. It is used as an antifungal antibiotic that is found to be useful both as the single agent and in combination with other agents in cancer treatment [96, 73, 143, 79, 123, 63, 64]. Current studies confirm the potent antitumor activity of TSA against breast cancer [157, 121, 3, 149, 160].

Colchicine is found in crocuses and primarily indicated to treat gout. It has been also used for treatment of familial mediterranean fever. A 12-year study in male patients with gout shows that patients who used Colchicine had a significantly lower risk of cancers than patients who never used Colchicine [77]. Another study in mice models shows that Colchicine can induce immunogenic cell death in tumor cells, suggesting the future clinical evaluation for Colchicine as a cancer vaccine [153]. Colchicine is reported to have an anticancer effect on human gastric cancer cell lines [82]. In particular, a recent study indicates that it can inhibit proliferation of the breast cancer MCF-7 cells and induce cell apoptosis, where the intensity of the effect depends on the time and dosage [141].

Tretinoin, all-trans-retinoic acid (ATRA), is the FDA-approved drug for the treatment of acne, photodamaged skin, and keratinization disorders. It is also used to treat acute promyelocytic leukemia (APL). The usefulness of ATRA in

treatment of breast cancer has been independently validated in study by Bhat-Nakshatri et al. [12]. Moreover, anti-proliferative, cyto-differentiating and apoptotic effects of ATRA are demonstrated in [40, 17, 142], suggesting the effectiveness of ATRA in treatment of breast cancer tumors with high retinoic acid receptor alpha (RARα) / retinoic acid receptor gamma (RARγ) ratios. Estrogen receptor-positive and Her2/neu-positive breast cancers are two subtypes of breast cancer that can be optimal targets for ATRA [83, 108].

Table 16 represents the target genes and activity of these drugs, obtained from KEGG and Drugbank [154].

Table 16: The FDA-approved drugs for breast cancer

Drug	Target genes	Activity
Fulvestrant	*ESR (1,2)*	Estrogen receptor antagonist
Methotrexate	*DHFR*	Antimetabolite
Paclitaxel	*BCL2*, *TUBB1*, *NR1I2*, *MAP (2,4)*, *MAPT*	Tubulin depolymerization inhibitor

Tables 18–23 show the results obtained on 6 breast cancer datasets using: i) the proposed approach, ii) the drug-disease approach, and iii) the anti-correlation approach. The FDA-approved drugs for breast cancer are highlighted in green. Interestingly, all two instances of Fulvestrant that are all exposures of the same cell line (MCF7) (with the same dosage) are highly ranked by our approach in all datasets. MCF7 cell line is an ideal model for hormone therapy that was established in 1973 at the Michigan Cancer Foundation [139].

We selected the top 5% drugs from the drugs ranked lists obtained by applying the proposed approach on 6 breast cancer datasets. These drugs are ranked according to the scores computed by the systematic method from the highest to the lowest. Table 17 shows the rank-ordered list of such drugs according to their score.

Table 17: The top 5% drugs obtained from the result of our repurposing approach. These drugs are ranked based on the scores generated by the systematic method. The * denotes the drugs that are currently FDA-approved but for other indications. Fulvestrant, Paclitaxel, and Methotrexate highlighted with green, are FDA-approved for the treatment of breast cancer. The sum of the scores assigned to these drugs is 0. Drugs with the same scores are sorted based on their average ranks in drugs ranked lists.

Drug	Score
Fulvestrant	1.33
Paclitaxel	0
Captopril *	-0.33
Methotrexate	-1.33
Glibenclamide *	-2
Fluorometholone *	-2.33
Clobetasol	-2.67
Trichostatin A	-2.83
Etoposide *	-3.33
Colchicine *	-3.67
Tretinoin *	-3.67
Alvespimycin	-3.67
Resveratrol	-3.67
Methylergometrine	-4

Table 18: A comparison between the results of three approaches: proposed, drug-disease, anti-correlation using GSE65194-Her2 dataset(the top 10 drugs). The p-values for Wilcoxon rank sum test comparing the results of the proposed approach with drug-disease and anti-correlation approaches are 0.01 and 0.02, respectively. Drugs highlighted with green are FDA-approved for the treatment of breast cancer. The * denotes the drugs that are currently FDA-approved but for other indications. Such drugs can be used off-label.

GSE65194-Her2 Proposed	Drug-disease	Anti-correlation
captopril_1988 *	glibenclamide_1546	glibenclamide_1546
paclitaxel_6720	danazol_2038 *	cimetidine_1884 *
fulvestrant_1630	cimetidine_1884 *	danazol_2038 *
fulvestrant_985	domperidone_2655	ajmaline_1749 *
etoposide_3241 *	trichostatin A_5017	domperidone_2655
captopril_4585 *	ipratropium bromide_1769	ipratropium bromide_1769
ipratropium bromide_1769	etoposide_3241 *	acepromazine_1777
metoclopramide_2353 *	ajmaline_1749 *	nilutamide_5362
domperidone_2655	methotrexate_5000	genistein_5232
methotrexate_5000	resveratrol_841 *	captopril_1988 *

Table 19: A comparison between the results of three approaches: proposed, drug-disease, anti-correlation using GSE65194-LuminalA dataset (the top 10 drugs).The p-values for Wilcoxon rank sum test comparing the results of the proposed approach with drug-disease and anti-correlation approaches are 0.03 and 0.04, respectively. Drugs highlighted with green are FDA-approved for the treatment of breast cancer. The * denotes the drugs that are currently FDA-approved but for other indications. The proposed approach was the only one who was able to rank the FDA-approved drugs in the top 10.

GSE65194-LuminalA Proposed	Drug-disease	Anti-correlation
fulvestrant_985	glibenclamide_1546 *	domperidone_2655
fulvestrant_1630	domperidone_2655	glibenclamide_1546 *
captopril_1988 *	cimetidine_1884 *	cimetidine_1884 *
fluorometholone_6247 *	danazol_2038 *	ipratropium bromide_1769
glibenclamide_1546 *	ipratropium bromide_1769	danazol_2038 *
captopril_4585 *	trichostatin A_5017	nilutamide_5362
paclitaxel_6720	nilutamide_5362 *	ajmaline_1749 *
vorinostat_6939 *	ethosuximide_1433 *	genistein_5232
cimetidine_1884 *	ajmaline_1749 *	acepromazine_1777
trichostatin A_5017	genistein_5232	ethosuximide_1433 *

Table 20: A comparison between the results of three approaches: proposed, drug-disease, anti-correlation using GSE65194-LuminalB dataset (the top 10 drugs). The p-values for Wilcoxon rank sum test comparing the results of the proposed approach with drug-disease and anti-correlation approaches are 0.02 and 0.01, respectively. Drugs highlighted with green are FDA-approved for the treatment of breast cancer. The * denotes the drugs that are currently FDA-approved but for other indications.

GSE65194-LuminalB Proposed	Drug-disease	Anti-correlation
fulvestrant_985	glibenclamide_1546 *	glibenclamide_1546 *
fulvestrant_1630	cimetidine_1884 *	cimetidine_1884 *
paclitaxel_6720	danazol_2038 *	danazol_2038 *
captopril_1988 *	ajmaline_1749 *	ajmaline_1749 *
trichostatin A_5017	trichostatin A_5017	domperidone_2655
phenelzine_4360 *	domperidone_2655	ipratropium bromide_1769
fluorometholone_6247 *	etoposide_3241 *	fluorometholone_6247 *
valproic acid_2700 *	ipratropium bromide_1769	sirolimus_1080 *
etoposide_3241 *	sirolimus_1080 *	acepromazine_1777
glibenclamide_1546 *	methotrexate_5000	nilutamide_5362

Table 21: A comparison between the results of three approaches: proposed, drug-disease, anti-correlation using GSE65194-Triple Negative dataset (the top 10 drugs). The p-values for Wilcoxon rank sum test comparing the results of the proposed approach with drug-disease and anti-correlation approaches are 0.03 and 0.007, respectively. Drugs highlighted with green are FDA-approved for the treatment of breast cancer. The * denotes the drugs that are currently FDA-approved but for other indications.

GSE65194-Triple Negative		
Proposed	Drug-disease	Anti-correlation
captopril_1988 *	glibenclamide_1546 *	glibenclamide_1546 *
paclitaxel_6720	danazol_2038 *	danazol_2038 *
etoposide_3241 *	cimetidine_1884 *	ajmaline_1749 *
clobetasol_6835	ajmaline_1749 *	cimetidine_1884 *
methotrexate_5000	methotrexate_5000	ipratropium bromide_1769
fulvestrant_985	resveratrol_841 *	domperidone_2655
glibenclamide_1546 *	ipratropium bromide_1769	acepromazine_1777
fulvestrant_1630	trichostatin A_5017	etoposide_3241 *
captopril_4585 *	acepromazine_1777	nilutamide_5362
domperidone_2655	wortmannin_1023 *	methotrexate_5000

Table 22: A comparison between the results of three approaches: proposed, drug-disease, anti-correlation using GSE28645 dataset (the top 10 drugs). The p-values for Wilcoxon rank sum test comparing the results of the proposed approach with drug-disease and anti-correlation approaches are 0.05 and 0.07, respectively. Drugs highlighted with green are FDA-approved for the treatment of breast cancer. The * denotes the drugs that are currently FDA-approved but for other indications.

GSE28645		
Proposed	Drug-disease	Anti-correlation
fulvestrant_985	paclitaxel_6720	phenelzine_4360 *
fulvestrant_1630	captopril_1988 *	valproic acid_1181 *
methylergometrine_1607	phenelzine_4360 *	paclitaxel_6720
alvespimycin_993	fluphenazine_6954 *	rosiglitazone_4457 *
colchicine_1598 *	clomipramine_4487 *	captopril_1988 *
captopril_1988 *	rosiglitazone_4457 *	troglitazone_4456 *
vorinostat_6939 *	genistein_5232	quercetin_2499
captopril_4585 *	astemizole_6807 *	hyoscyamine_1424 *
sirolimus_1080 *	chlorpromazine_5074 *	clomipramine_4487 *
trichostatin A_5017	cimetidine_1884 *	genistein_1176

Table 23: A comparison between the results of three approaches: proposed, drug-disease, anti-correlation using GSE1299 dataset (the top 10 drugs). The p-values for Wilcoxon rank sum test comparing the results of the proposed approach with drug-disease and anti-correlation approaches are 0.007 and 0.02, respectively. Drugs highlighted with green are FDA-approved for the treatment of breast cancer. The * denotes the drugs that are currently FDA-approved but for other indications.

GSE1299 Proposed	Drug-disease	Anti-correlation
methotrexate_5419	etoposide_3241 *	etoposide_3241 *
resveratrol_841 *	ciclopirox_3317 *	valproic acid_1181 *
methotrexate_5000	resveratrol_841 *	rifabutin_4349 *
fulvestrant_985	valproic acid_1181 *	methotrexate_5419
tretinoin_6170 *	rifabutin_4349 *	resveratrol_841 *
phenelzine_4360 *	ivermectin_2213 *	rifabutin_3873 *
fulvestrant_1630	oxyphenbutazone_6844	ciclopirox_3317 *
tretinoin_1548 *	methotrexate_5419	prochlorperazine_5212 *
troglitazone_4456 *	rifabutin_3873 *	vorinostat_6939 *
rosiglitazone_4457 *	wortmannin_1023 *	phenelzine_4360 *

References

[1] A. Abdollahi, M. Li, G. Ping, C. Plathow, S. Domhan, F. Kiessling, L. B. Lee, G. McMahon, H.-J. Gröne, K. E. Lipson, et al. Inhibition of platelet-derived growth factor signaling attenuates pulmonary fibrosis. *The Journal of Experimental Medicine*, 201(6):925–935, 2005.

[2] M. Abdul and N. Hoosein. Expression and activity of potassium ion channels in human prostate cancer. *Cancer Letters*, 186(1):99–105, 2002.

[3] J. P. Alao, A. V. Stavropoulou, E. W. Lam, R. C. Coombes, and D. M. Vigushin. Histone deacetylase inhibitor, trichostatin a induces ubiquitin-dependent cyclin d1 degradation in mcf-7 breast cancer cells. *Molecular Cancer*, 5(1):8, 2006.

[4] J. T. Allen and M. A. Spiteri. Growth factors in mocetinostat pulmonary fibrosis: relative roles. *Respiratory Research*, 3(1):1, 2001.

[5] R. J. Amato, J. Jac, T. Mohammad, and S. Saxena. Pilot study of rapamycin in patients with hormone-refractory prostate cancer. *Clinical Genitourinary Cancer*, 6(2):97–102, 2008.

[6] H. Antoniades, M. Bravo, R. Avila, T. Galanopoulos, J. Neville-Golden, M. Maxwell, and M. Selman. Platelet-derived growth factor in mocetinostat pulmonary fibrosis. *Journal of Clinical Investigation*, 86(4):1055, 1990.

[7] M. Ashburner, C. A. Ball, J. A. Blake, D. Botstein, H. Butler, J. M. Cherry, A. P. Davis, K. Dolinski, S. S. Dwight, J. T. Eppig, M. A. Harris, D. P. Hill, L. Issel-Tarver, A. Kasarskis, S. Lewis, J. C. Matese, J. E. Richardson, M. Ringwald, G. M. Rubin, and G. Sherlock. Gene Ontology: tool for the unification of biology. *Nature Genetics*, 25:25–29, 2000.

[8] D. M. Atienza, C. L. Vogel, B. Trock, and S. M. Swain. Phase II study of oral etoposide for patients with advanced breast cancer. *Cancer*, 76(12):2485–2490, 1995.

[9] C. P. Baran, J. M. Opalek, S. McMaken, C. A. Newland, J. M. O'Brien Jr, M. G. Hunter, B. D. Bringardner, M. M. Monick, D. R. Brigstock, P. C. Stromberg, et al. Important roles for macrophage colony-stimulating factor, cc chemokine ligand 2, and mononuclear phagocytes in the pathogenesis of pulmonary fibrosis. *American Journal of Respiratory and Critical Care Medicine*, 176(1):78–89, 2007.

[10] C. Behrens, H. Y. Lin, J. J. Lee, M. G. Raso, W. K. Hong, I. I. Wistuba, and R. Lotan. Immunohistochemical expression of basic fibroblast growth

factor and fibroblast growth factor receptors 1 and 2 in the pathogenesis of lung cancer. *Clinical Cancer Research*, 14(19):6014–6022, 2008.

[11] S. Benzina, J. Harquail, S. Jean, A.-P. Beauregard, C. D Colquhoun, M. Carroll, A. Bos, C. A Gray, and G. A Robichaud. Deoxypodophyllotoxin isolated from juniperus communis induces apoptosis in breast cancer cells. *Anti-Cancer Agents in Medicinal Chemistry (Formerly Current Medicinal Chemistry-Anti-Cancer Agents)*, 15(1):79–88, 2015.

[12] P. Bhat-Nakshatri, C. P. Goswami, S. Badve, G. W. Sledge Jr, and H. Nakshatri. Identification of FDA-approved drugs targeting breast cancer stem cells along with biomarkers of sensitivity. *Scientific Reports*, 3:2530, 2013.

[13] N. Bilani, H. Bahmad, and W. Abou-Kheir. Prostate cancer and aspirin use: Synopsis of the proposed molecular mechanisms. *Frontiers in pharmacology*, 8:145, 2017.

[14] D. J. Boffa, F. Luan, D. Thomas, H. Yang, V. K. Sharma, M. Lagman, and M. Suthanthiran. Rapamycin inhibits the growth and metastatic progression of non-small cell lung cancer. *Clinical Cancer Research*, 10(1):293–300, 2004.

[15] D. Bradley, D. Rathkopf, R. Dunn, W. M. Stadler, G. Liu, D. C. Smith, R. Pili, J. Zwiebel, H. Scher, and M. Hussain. Vorinostat in advanced prostate cancer patients progressing on prior chemotherapy (national cancer institute trial 6862). *Cancer*, 115(23):5541–5549, 2009.

[16] B. D. Bringardner, C. P. Baran, T. D. Eubank, and C. B. Marsh. The role of inflammation in the pathogenesis of idiopathic pulmonary fibrosis. *Antioxidants & Redox Signaling*, 10(2):287–302, 2008.

[17] G. T. Budd, P. C. Adamson, M. Gupta, P. Homayoun, S. K. Sandstrom, R. F. Murphy, D. McLain, L. Tuason, D. Peereboom, R. M. Bukowski, et al. Phase I/II trial of all-trans retinoic acid and tamoxifen in patients with advanced breast cancer. *Clinical Cancer Research*, 4(3):635–642, 1998.

[18] B. Cao, Z. Guo, Y. Zhu, and W. Xu. The potential role of PDGF, IGF-1, TGF-*beta* expression in mocetinostat pulmonary fibrosis. *Chinese Medical Journal*, 113(9):776–782, 2000.

[19] S. L. Carter, M. M. Centenera, W. D. Tilley, L. A. Selth, and L. M. Butler. Iκbα mediates prostate cancer cell death induced by combinatorial targeting of the androgen receptor. *BMC Cancer*, 16(1):141, 2016.

[20] K. Chamie, P. Ghosh, T. Koppie, V. Romero, C. Troppmann, and R. deVere White. The effect of sirolimus on prostate-specific antigen (psa) levels in male renal transplant recipients without prostate cancer. *American Journal of Transplantation*, 8(12):2668–2673, 2008.

[21] U. R. Chandran, C. Ma, R. Dhir, M. Bisceglia, M. Lyons-Weiler, W. Liang, G. Michalopoulos, M. Becich, and F. A. Monzon. Gene expression profiles of prostate cancer reveal involvement of multiple molecular pathways in the metastatic process. *BMC Cancer*, 7(1):64, 2007.

[22] B. H. Chao, R. Briesewitz, and M. A. Villalona-Calero. RET fusion genes in non–small-cell lung cancer. *Journal of Clinical Oncology*, 30(35):4439–4441, 2012.

[23] A. Chase, C. Bryant, J. Score, and N. C. Cross. Ponatinib as targeted therapy for fgfr1 fusions associated with the 8p11 myeloproliferative syndrome. *Haematologica*, 98(1):103–106, 2013.

[24] N. Chaudhary, G. Roth, F. Hilberg, J. Müller-Quernheim, A. Prasse, G. Zissel, A. Schnapp, and J. Park. Inhibition of PDGF, VEGF and FGF signalling attenuates fibrosis. *European Respiratory Journal*, 29(5):976–985, 2007.

[25] J.-Y. Chen, Y.-A. Tang, W.-S. Li, Y.-C. Chiou, J.-M. Shieh, and Y.-C. Wang. A synthetic podophyllotoxin derivative exerts anti-cancer effects by inducing mitotic arrest and pro-apoptotic ER stress in lung cancer preclinical models. *PloS One*, 8(4):e62082, 2013.

[26] L. Chen, C. Chu, J. Lu, X. Kong, T. Huang, and Y.-D. Cai. Gene ontology and kegg pathway enrichment analysis of a drug target-based classification system. *PloS One*, 10(5):e0126492, 2015.

[27] J.-H. Cho, R. Gelinas, K. Wang, A. Etheridge, M. G. Piper, K. Batte, D. Dakhlallah, J. Price, D. Bornman, S. Zhang, et al. Systems biology of interstitial lung diseases: integration of mRNA and microRNA expression changes. *BMC Medical Genomics*, 4(1):1, 2011.

[28] K. S. Choe, J. E. Cowan, J. M. Chan, P. R. Carroll, A. V. D'Amico, and S. L. Liauw. Aspirin use and the risk of prostate cancer mortality in men treated with prostatectomy or radiotherapy. *Journal of Clinical Oncology*, 30(28):3540–3544, 2012.

[29] J. Y. Choi, W. G. Hong, J. H. Cho, E. M. Kim, J. Kim, C.-H. Jung, S.-G. Hwang, H.-D. Um, and J. K. Park. Podophyllotoxin acetate triggers anticancer effects against non-small cell lung cancer cells by promoting cell

death via cell cycle arrest, ER stress and autophagy. *International Journal of Oncology*, 47(4):1257–1265, 2015.

[30] C. Ciccarese, F. Massari, R. Iacovelli, M. Fiorentino, R. Montironi, V. Di Nunno, F. Giunchi, M. Brunelli, and G. Tortora. Prostate cancer heterogeneity: Discovering novel molecular targets for therapy. *Cancer Treatment Reviews*, 2017.

[31] J. Cicenas, K. Kalyan, A. Sorokinas, E. Stankunas, J. Levy, I. Meskinyte, V. Stankevicius, A. Kaupinis, and M. Valius. Roscovitine in cancer and other diseases. *Annals of Translational Medicine*, 3(10), 2015.

[32] A. S. Clark, K. A. West, P. M. Blumberg, and P. A. Dennis. Altered protein kinase c (PKC) isoforms in non-small cell lung cancer cells. *Cancer Research*, 63(4):780–786, 2003.

[33] S. Dakshanamurthy, N. T. Issa, S. Assefnia, A. Seshasayee, O. J. Peters, S. Madhavan, A. Uren, M. L. Brown, and S. W. Byers. Predicting new indications for approved drugs using a proteo-chemometric method. *Journal of Medicinal Chemistry*, 55(15):6832, 2012.

[34] S. Detchokul and A. G. Frauman. Recent developments in prostate cancer biomarker research: therapeutic implications. *British Journal of Clinical Pharmacology*, 71(2):157–174, 2011.

[35] S. Drăghici, P. Khatri, A. L. Tarca, K. Amin, A. Done, C. Voichiţa, C. Georgescu, and R. Romero. A systems biology approach for pathway level analysis. *Genome Research*, 17(10):1537–1545, 2007.

[36] R. Edgar, M. Domrachev, and A. E. Lash. Gene Expression Omnibus: NCBI gene expression and hybridization array data repository. *Nucleic Acids Research*, 30(1):207–210, 2002.

[37] S. Ekman, M. W. Wynes, and F. R. Hirsch. The mTOR pathway in lung cancer and implications for therapy and biomarker analysis. *Journal of Thoracic Oncology*, 7(6):947–953, 2012.

[38] A. Franceschini, D. Szklarczyk, S. Frankild, M. Kuhn, M. Simonovic, A. Roth, J. Lin, P. Minguez, P. Bork, C. Von Mering, et al. String v9. 1: protein-protein interaction networks, with increased coverage and integration. *Nucleic Acids Research*, 41(D1):D808–D815, 2013.

[39] J. F. Gainor and A. T. Shaw. Novel targets in non-small cell lung cancer: ROS1 and RET fusions. *The Oncologist*, 18(7):865–875, 2013.

[40] E. Garattini, G. Paroni, and M. Terao. Retinoids and breast cancer: new clues to increase their activity and selectivity. *Breast Cancer Research*, 14(5):1, 2012.

[41] O. Gautschi, J. Milia, T. Filleron, J. Wolf, D. P. Carbone, D. Owen, R. Camidge, V. Narayanan, R. C. Doebele, B. Besse, et al. Targeting RET in patients with RET-rearranged lung cancers: Results from the global, multicenter RET registry. *Journal of Clinical Oncology*, 35(13):1403–1410, 2017.

[42] Y. Geng, L. Kohli, B. J. Klocke, and K. A. Roth. Chloroquine-induced autophagic vacuole accumulation and cell death in glioma cells is p53 independent. *Neuro-oncology*, 12(5):473–481, 2010.

[43] A. . Goldhirsch, W. C. Wood, A. S. Coates, R. D. Gelber, B. Thürlimann, H.-J. Senn, and P. members. Strategies for subtypes?dealing with the diversity of breast cancer: highlights of the st gallen international expert consensus on the primary therapy of early breast cancer 2011. *Annals of oncology*, 22(8):1736–1747, 2011.

[44] M. Gordaliza, M. d. Castro, J. Miguel del Corral, and A. S. Feliciano. Antitumor properties of podophyllotoxin and related compounds. *Current Pharmaceutical Design*, 6(18):1811–1839, 2000.

[45] T. Goto, H. Matsushima, Y. Kasuya, Y. Hosaka, T. Kitamura, K. Kawabe, A. Hida, Y. Ohta, T. Simizu, and K. Takeda. The effect of papaverine on morphologic differentiation, proliferation and invasive potential of human prostatic cancer lncap cells. *International Journal of Urology*, 6(6):314–319, 1999.

[46] C. Gridelli, P. Maione, and A. Rossi. The potential role of mTOR inhibitors in non-small cell lung cancer. *The Oncologist*, 13(2):139–147, 2008.

[47] F. Grimminger, A. Günther, and C. Vancheri. The role of tyrosine kinases in the pathogenesis of mocetinostat pulmonary fibrosis. *European Respiratory Journal*, 51:ERJ–01496, 2015.

[48] F. Grimminger, R. T. Schermuly, and H. A. Ghofrani. Targeting non-malignant disorders with tyrosine kinase inhibitors. *Nature Reviews Drug Discovery*, 9(12):956–970, 2010.

[49] L. A. Habel, W. Zhao, and J. L. Stanford. Daily aspirin use and prostate cancer risk in a large, multiracial cohort in the us. *Cancer Causes and Control*, 13(5):427–434, 2002.

[50] M. Haigentz Jr, J. Nemunaitis, M. Johnson, N. Mohindra, K. Eaton, M. Patel, M. Awad, D. Briere, N. Sudhakar, D. Faltaos, et al. Phase 1/2 study of mocetinostat and durvalumab (medi4736) in patients with advanced solid tumors and non-small cell lung cancer (NSCLC). In *Journal of Thoracic Oncology*, volume 12, pages S1073–S1074. ELSEVIER SCIENCE INC 360 PARK AVE SOUTH, NEW YORK, NY 10010-1710 USA, 2017.

[51] F. Hilberg, G. J. Roth, M. Krssak, S. Kautschitsch, W. Sommergruber, U. Tontsch-Grunt, P. Garin-Chesa, G. Bader, A. Zoephel, J. Quant, et al. BIBF 1120: triple angiokinase inhibitor with sustained receptor blockade and good antitumor efficacy. *Cancer Research*, 68(12):4774–4782, 2008.

[52] S. Homma, I. Nagaoka, H. Abe, K. Takahashi, K. Seyama, T. Nukiwa, and S. Kira. Localization of platelet-derived growth factor and insulin-like growth factor I in the fibrotic lung. *American Journal of Respiratory and Critical Care Medicine*, 152(6):2084–2089, 1995.

[53] A. L. Hopkins. Network pharmacology: the next paradigm in drug discovery. *Nature Chemical Biology*, 4(11):682–690, 2008.

[54] A. L. Hopkins et al. Network pharmacology. *Nature Biotechnology*, 25(10):1110–1110, 2007.

[55] S. Hu, Q. Zhou, W.-R. Wu, Y.-X. Duan, Z.-Y. Gao, Y.-W. Li, and Q. Lu. Anticancer effect of deoxypodophyllotoxin induces apoptosis of human prostate cancer cells. *Oncology Letters*, 12(4):2918–2923, 2016.

[56] D. W. Huang, B. T. Sherman, and R. A. Lempicki. Bioinformatics enrichment tools: paths toward the comprehensive functional analysis of large gene lists. *Nucleic Acids Research*, 37(1):1–13, 2009.

[57] D. W. Huang, B. T. Sherman, and R. A. Lempicki. Systematic and integrative analysis of large gene lists using david bioinformatics resources. *Nature Protocols*, 4(1):44–57, 2009.

[58] H. Huang, L.-J. Li, H.-B. Zhang, and A.-Y. Wei. Papaverine selectively inhibits human prostate cancer cell (PC-3) growth by inducing mitochondrial mediated apoptosis, cell cycle arrest and downregulation of nf-κb/pi3k/akt signalling pathway. *Journal of BU ON.: Official Journal of the Balkan Union of Oncology*, 22(1):112, 2017.

[59] A. Imrali, X. Mao, M. Yeste-Velasco, J. Shamash, and Y. Lu. Rapamycin inhibits prostate cancer cell growth through cyclin D1 and enhances the cytotoxic efficacy of cisplatin. *American Journal of Cancer Research*, 6(8):1772, 2016.

[60] R. A. Irizarry, B. Hobbs, F. Collin, Y. D. Beazer-Barclay, K. J. Antonellis, U. Scherf, and T. P. Speed. Exploration, Normalization, and Summaries of High Density Oligonucleotide Array Probe Level Data. *Biostatistics*, 4(2):249–264, 2003.

[61] N. T. Issa, J. Kruger, H. Wathieu, R. Raja, S. W. Byers, and S. Dakshanamurthy. Druggenex-net: a novel computational platform for systems pharmacology and gene expression-based drug repurposing. *BMC Bioinformatics*, 17(1):202, 2016.

[62] E. J. Jacobs, C. Rodriguez, A. M. Mondul, C. J. Connell, S. J. Henley, E. E. Calle, and M. J. Thun. A large cohort study of aspirin and other nonsteroidal anti-inflammatory drugs and prostate cancer incidence. *Journal of the National Cancer Institute*, 97(13):975–980, 2005.

[63] E. R. Jang, S.-J. Lim, E. S. Lee, G. Jeong, T.-Y. Kim, Y.-J. Bang, and J.-S. Lee. The histone deacetylase inhibitor trichostatin a sensitizes estrogen receptor α-negative breast cancer cells to tamoxifen. *Oncogene*, 23(9):1724–1736, 2004.

[64] X. Jin, Y. Fang, Y. Hu, J. Chen, W. Liu, G. Chen, M. Gong, P. Wu, T. Zhu, S. Wang, et al. Synergistic activity of the histone deacetylase inhibitor trichostatin a and the proteasome inhibitor ps-341 against taxane-resistant ovarian cancer cell lines. *Oncology Letters*, 13(6):4619–4626, 2017.

[65] P. Jones, K. Christodoulos, N. Dobbs, P. Thavasu, F. Balkwill, A. Blann, G. Caine, S. Kumar, A. Kakkar, N. Gompertz, et al. Combination antiangiogenesis therapy with marimastat, captopril and fragmin in patients with advanced cancer. *British Journal of Cancer*, 91(1):30–36, 2004.

[66] S. Karmakar, Y. Jin, and A. K. Nagaich. Interaction of glucocorticoid receptor (GR) with estrogen receptor (er) α and activator protein 1 (AP1) in dexamethasone-mediated interference of ERα activity. *Journal of Biological Chemistry*, 288(33):24020–24034, 2013.

[67] W. Kassouf, S. Tanguay, and A. G. Aprikian. Nilutamide as second line hormone therapy for prostate cancer after androgen ablation fails. *The Journal of Urology*, 169(5):1742–1744, 2003.

[68] R. E. Kast and M.-E. Halatsch. Matrix metalloproteinase-2 and-9 in glioblastoma: A trio of old drugs–captopril, disulfiram and nelfinavir–are inhibitors with potential as adjunctive treatments in glioblastoma. *Archives of Medical Research*, 43(3):243–247, 2012.

[69] D. Kaushik, V. Vashistha, S. Isharwal, S. A. Sediqe, and M.-F. Lin. Histone deacetylase inhibitors in castration-resistant prostate cancer: molecular mechanism of action and recent clinical trials. *Therapeutic Advances in Urology*, 7(6):388–395, 2015.

[70] G. M. Keating. Nintedanib: a review of its use in patients with mocetinostat pulmonary fibrosis. *Drugs*, 75(10):1131–1140, 2015.

[71] B. D. Keith. Systematic review of the clinical effect of glucocorticoids on nonhematologic malignancy. *BMC Cancer*, 8(1):84, 2008.

[72] P. Khatri, M. Sirota, and A. J. Butte. Ten years of pathway analysis: current approaches and outstanding challenges. *PLoS Computational Biology*, 8(2):e1002375, 2012.

[73] H.-J. Kim and S.-C. Bae. Histone deacetylase inhibitors: molecular mechanisms of action and clinical trials as anti-cancer drugs. *American Journal of Translational Research*, 3(2):166, 2011.

[74] K.-Y. Kim, H.-J. Cho, S.-N. Yu, S.-H. Kim, H.-S. Yu, Y.-M. Park, N. Mirkheshti, S. Y. Kim, C. S. Song, B. Chatterjee, et al. Interplay of reactive oxygen species, intracellular ca2+ and mitochondrial homeostasis in the apoptosis of prostate cancer cells by deoxypodophyllotoxin. *Journal of Cellular Biochemistry*, 114(5):1124–1134, 2013.

[75] D. Knoerzer, T. Baginski, K. Wade, C. Fan, S. Rapp, K. Regina, F. Shih, M. Burney, S. Rouw, and D. Welsch. Therapeutic efficacy of Sunitinib and other broad spectrum receptor tyrosine kinase inhibitors (RTKI) in bleomycin-induced pulmonary fibrosis. *Journal of Inflammation*, 10(1):1, 2013.

[76] B. Krusche, J. Arend, and T. Efferth. Synergistic inhibition of angiogenesis by artesunate and captopril in vitro and in vivo. *Evidence-Based Complementary and Alternative Medicine*, 2013, 2013.

[77] M.-C. Kuo, S.-J. Chang, and M.-C. Hsieh. Colchicine significantly reduces incident cancer in gout male patients: a 12-year cohort study. *Medicine*, 94(50), 2015.

[78] J. Lamb, E. D. Crawford, D. Peck, J. W. Modell, I. C. Blat, M. J. Wrobel, J. Lerner, J.-P. Brunet, A. Subramanian, K. N. Ross, et al. The connectivity map: using gene-expression signatures to connect small molecules, genes, and disease. *Science*, 313(5795):1929–1935, 2006.

[79] A. A. Lane and B. A. Chabner. Histone deacetylase inhibitors in cancer therapy. *Journal of Clinical Oncology*, 27(32):5459–5468, 2009.

[80] Q. Li, T. Cheng, Y. Wang, and S. H. Bryant. Pubchem as a public resource for drug discovery. *Drug Discovery Today*, 15(23):1052–1057, 2010.

[81] K.-T. Lin and L.-H. Wang. New dimension of glucocorticoids in cancer treatment. *Steroids*, 111:84–88, 2016.

[82] Z.-Y. Lin, C.-H. Kuo, D.-C. Wu, and W.-L. Chuang. Anticancer effects of clinically acceptable colchicine concentrations on human gastric cancer cell lines. *The Kaohsiung Journal of Medical Sciences*, 32(2):68–73, 2016.

[83] M. Lu, R. Mira-y Lopez, S. Nakajo, K. Nakaya, and Y. Jing. Expression of estrogen receptor α, retinoic acid receptor α and cellular retinoic acid binding protein II genes is coordinately regulated in human breast cancer cells. *Oncogene*, 24(27):4362–4369, 2005.

[84] D. Ma, B. Lu, C. Feng, C. Wang, Y. Wang, T. Luo, J. Feng, H. Jia, G. Chi, Y. Luo, and P. Ge. Deoxypodophyllotoxin triggers parthanatos in glioma cells via induction of excessive ROS. *Cancer Letters*, 371(2):194–204, 2016.

[85] Y. Ma and N. Brusselaers. Maintenance use of aspirin or other non-steroidal anti-inflammatory drugs (nsaids) and prostate cancer risk. *Prostate Cancer and Prostatic Diseases*, page 1, 2017.

[86] S. K. Madala, S. Schmidt, C. Davidson, M. Ikegami, S. Wert, and W. D. Hardie. MEK-ERK pathway modulation ameliorates pulmonary fibrosis associated with epidermal growth factor receptor activation. *American Journal of Respiratory Cell and Molecular Biology*, 46(3):380–388, 2012.

[87] T. Madej, K. J. Addess, J. H. Fong, L. Y. Geer, R. C. Geer, C. J. Lanczycki, C. Liu, S. Lu, A. Marchler-Bauer, A. R. Panchenko, et al. Mmdb: 3d structures and macromolecular interactions. *Nucleic Acids Research*, 40(D1):D461–D464, 2012.

[88] V. Maire, C. Baldeyron, M. Richardson, B. Tesson, A. Vincent-Salomon, E. Gravier, B. Marty-Prouvost, L. De Koning, G. Rigaill, A. Dumont, et al. TTK/hMPS1 is an attractive therapeutic target for triple-negative breast cancer. *PloS One*, 8(5):e63712, 2013.

[89] V. Maire, F. Némati, M. Richardson, A. Vincent-Salomon, B. Tesson, G. Rigaill, E. Gravier, B. Marty-Prouvost, L. De Koning, G. Lang, et al. Polo-like kinase 1: a potential therapeutic option in combination with conventional chemotherapy for the management of patients with triple-negative breast cancer. *Cancer Research*, 73(2):813–823, 2013.

[90] C. Mattingly, M. Rosenstein, G. Colby, J. Forrest Jr, and J. Boyer. The comparative toxicogenomics database (CTD): a resource for comparative

toxicological studies. *Journal of Experimental Zoology Part A: Comparative Experimental Biology*, 305(9):689–692, 2006.

[91] S. Maubant, B. Tesson, V. Maire, M. Ye, G. Rigaill, D. Gentien, F. Cruzalegui, G. C. Tucker, S. Roman-Roman, and T. Dubois. Transcriptome analysis of Wnt3a-treated triple-negative breast cancer cells. *PloS One*, 10(4):e0122333, 2015.

[92] M. E. Mazzei, L. Richeldi, and H. R. Collard. Nintedanib in the treatment of mocetinostat pulmonary fibrosis. *Therapeutic Advances in Respiratory Disease*, 9(3):121–129, 2015.

[93] B. H. Mecham, G. T. Klus, J. Strovel, M. Augustus, D. Byrne, P. Bozso, D. Z. Wetmore, T. J. Mariani, I. S. Kohane, and Z. Szallasi. Sequence-matched probes produce increased cross-platform consistency and more reproducible biological results in microarray-based gene expression measurements. *Nucleic Acids Research*, 32(9):e74, 2004.

[94] E. B. Meltzer, W. T. Barry, T. A. D'Amico, R. D. Davis, S. S. Lin, M. W. Onaitis, L. D. Morrison, T. A. Sporn, M. P. Steele, and P. W. Noble. Bayesian probit regression model for the diagnosis of pulmonary fibrosis: proof-of-principle. *BMC Medical Genomics*, 4(1):1, 2011.

[95] C. Mitrea, Z. Taghavi, B. Bokanizad, S. Hanoudi, R. Tagett, M. Donato, C. Voichiţa, and S. Drăghici. Methods and approaches in the topology-based analysis of biological pathways. *Frontiers in Physiology*, 4:278, 2013.

[96] M. Mottamal, S. Zheng, T. L. Huang, and G. Wang. Histone deacetylase inhibitors in clinical studies as templates for new anticancer agents. *Molecules*, 20(3):3898–3941, 2015.

[97] E. Nakajima, B. Helfrich, D. Chan, Z. Zhang, F. Hirsch, V. Chen, D. Ma, and P. Bunn Jr. Enzastaurin a protein kinase cbeta-selective inhibitor, inhibits the growth of sclc and nsclc cell lines. *Journal of Clinical Oncology*, 24(18_suppl):13138–13138, 2006.

[98] S. Namazi, J. Rostami-Yalmeh, E. Sahebi, M. Jaberipour, M. Razmkhah, and A. Hosseini. The role of captopril and losartan in prevention and regression of tamoxifen-induced resistance of breast cancer cell line MCF-7: an in vitro study. *Biomedicine & Pharmacotherapy*, 68(5):565–571, 2014.

[99] J. W. Neal and L. V. Sequist. Complex role of histone deacetylase inhibitors in the treatment of non–small-cell lung cancer. *Journal of Clinical Oncology*, 30(18):2280–2282, 2012.

[100] J. Nelson and R. E. Harris. Inverse association of prostate cancer and non-steroidal anti-inflammatory drugs (NSAIDs): results of a case-control study. *Oncology Reports*, 7(1):169–239, 2000.

[101] S. Novello, C. Camps, F. Grossi, J. Mazieres, L. Abrey, J.-M. Vernejoux, A. Thall, S. Patyna, T. Usari, Z. Wang, et al. Phase II study of sunitinib in patients with non-small cell lung cancer and irradiated brain metastases. *Journal of Thoracic Oncology*, 6(7):1260–1266, 2011.

[102] M. Núñez, V. Medina, G. Cricco, M. Croci, C. Cocca, E. Rivera, R. Bergoc, and G. Martín. Glibenclamide inhibits cell growth by inducing g0/g1 arrest in the human breast cancer cell line mda-mb-231. *BMC Pharmacology and Toxicology*, 14(1):6, 2013.

[103] Y. Oh, R. S. Herbst, H. Burris, A. Cleverly, L. Musib, M. Lahn, and G. Bepler. Enzastaurin, an oral serine/threonine kinase inhibitor, as second-or third-line therapy of non–small-cell lung cancer. *Journal of Clinical Oncology*, 26(7):1135–1141, 2008.

[104] K. C. Olsen, A. P. Epa, A. A. Kulkarni, R. M. Kottmann, C. E. McCarthy, G. V. Johnson, T. H. Thatcher, R. P. Phipps, and P. J. Sime. Inhibition of transglutaminase 2, a novel target for pulmonary fibrosis, by two small electrophilic molecules. *American Journal of Respiratory Cell and Molecular Biology*, 50(4):737–747, 2014.

[105] P. Ong, L. Wang, D. Chia, et al. A novel combinatorial strategy using Seliciclib® and belinostat® for eradication of non-small cell lung cancer via apoptosis induction and BID activation. *Cancer Letters*, 381(1):49–57, 2016.

[106] J. P. Overington, B. Al-Lazikani, and A. L. Hopkins. How many drug targets are there? *Nature Reviews Drug Discovery*, 5(12):993–996, 2006.

[107] Y. Pan, T. Cheng, Y. Wang, and S. H. Bryant. Pathway analysis for drug repositioning based on public database mining. *Journal of Chemical Information and Modeling*, 54(2):407–418, 2014.

[108] G. Paroni, M. Fratelli, G. Gardini, C. Bassano, M. Flora, A. Zanetti, V. Guarnaccia, P. Ubezio, F. Centritto, M. Terao, et al. Synergistic antitumor activity of lapatinib and retinoids on a novel subtype of breast cancer with coamplification of ERBB2 and RARA. *Oncogene*, 31(29):3431–3443, 2012.

[109] L. Payen, L. Delugin, A. Courtois, Y. Trinquart, A. Guillouzo, and O. Fardel. The sulphonylurea glibenclamide inhibits multidrug resistance

protein (mrp1) activity in human lung cancer cells. *British Journal of Pharmacology*, 132(3):778–784, 2001.

[110] H. Peng, F. Long, and C. Ding. Feature selection based on mutual information criteria of max-dependency, max-relevance, and min-redundancy. *IEEE Transactions on Pattern Analysis and Machine Intelligence*, 27(8):1226–1238, 2005.

[111] R. Peng, S. Sridhar, G. Tyagi, J. E. Phillips, R. Garrido, P. Harris, L. Burns, L. Renteria, J. Woods, L. Chen, et al. Bleomycin induces molecular changes directly relevant to mocetinostat pulmonary fibrosis: a model for "active" disease. *PloS One*, 8(4):e59348, 2013.

[112] A. Planche, M. Bacac, P. Provero, C. Fusco, M. Delorenzi, J.-C. Stehle, and I. Stamenkovic. Identification of prognostic molecular features in the reactive stroma of human breast and prostate cancer. *PloS One*, 6(5):18640, 2011.

[113] K. A. Price, C. G. Azzoli, L. M. Krug, M. C. Pietanza, N. A. Rizvi, W. Pao, M. G. Kris, G. J. Riely, R. T. Heelan, M. E. Arcila, et al. Phase II trial of gefitinib and everolimus in advanced non-small cell lung cancer. *Journal of Thoracic Oncology*, 5(10):1623–1629, 2010.

[114] X. Qian, J. Li, J. Ding, Z. Wang, L. Duan, and G. Hu. Glibenclamide exerts an antitumor activity through reactive oxygen species–c-jun nh (2)-terminal kinase pathway in human gastric cancer cell line mgc-803. *Biochemical Pharmacology*, 76(12):1705–1715, 2008.

[115] G. Raghu and M. Selman. Nintedanib and Pirfenidone. new antifibrotic treatments indicated for mocetinostat pulmonary fibrosis offer hopes and raises questions. *American Journal of Respiratory and Critical Care Medicine*, 191(3):252–254, 2015.

[116] J. S. Rai, M. J. Henley, and H. L. Ratan. Mammalian target of rapamycin: a new target in prostate cancer. In *Urologic Oncology: Seminars and Original Investigations*, volume 28, pages 134–138. Elsevier, 2010.

[117] A. S. Reddy and S. Zhang. Polypharmacology: drug discovery for the future. *Expert Review of Clinical Pharmacology*, 6(1):41–47, 2013.

[118] M. Ren, M. Hong, G. Liu, H. Wang, V. Patel, P. Biddinger, J. Silva, J. Cowell, and Z. Hao. Novel fgfr inhibitor ponatinib suppresses the growth of non-small cell lung cancer cells overexpressing fgfr1. *Oncology Reports*, 29(6):2181–2190, 2013.

[119] E. A. Renzoni, D. J. Abraham, S. Howat, X. Shi-Wen, P. Sestini, G. Bou-Gharios, A. U. Wells, S. Veeraraghavan, A. G. Nicholson, C. P. Denton, et al. Gene expression profiling reveals novel TGFβ targets in adult lung fibroblasts. *Respiratory Research*, 5(1):24, 2004.

[120] C. K. Rhee, S. H. Lee, H. K. Yoon, S. C. Kim, S. Y. Lee, S. S. Kwon, Y. K. Kim, K. H. Kim, T. J. Kim, and J. W. Kim. Effect of nilotinib on bleomycin-induced acute lung injury and pulmonary fibrosis in mice. *Respiration*, 82(3):273–287, 2011.

[121] L. V. Rhodes, A. M. Nitschke, H. C. Segar, E. C. Martin, J. L. Driver, S. Elliott, S. Y. Nam, M. Li, K. P. Nephew, M. E. Burow, et al. The histone deacetylase inhibitor trichostatin a alters microrna expression profiles in apoptosis-resistant breast cancer cells. *Oncology Reports*, 27(1):10–16, 2012.

[122] L. Richeldi, U. Costabel, M. Selman, D. S. Kim, D. M. Hansell, A. G. Nicholson, K. K. Brown, K. R. Flaherty, P. W. Noble, G. Raghu, M. Brun, A. Gupta, N. Juhel, M. Klüglich, and R. M. Bois. Efficacy of a tyrosine kinase inhibitor in mocetinostat pulmonary fibrosis. *New England Journal of Medicine*, 365(12):1079–1087, 2011.

[123] M. Roh, C. Kim, B. Park, G. Kim, J. Jeong, H. Kwon, D. Suh, K. Cho, S.-B. Yee, and Y. Yoo. Mechanism of histone deacetylase inhibitor trichostatin a induced apoptosis in human osteosarcoma cells. *Apoptosis*, 9(5):583–589, 2004.

[124] Z. Rong, L. Li, F. Fei, L. Luo, and Y. Qu. Combined treatment of glibenclamide and cocl2 decreases mmp9 expression and inhibits growth in highly metastatic breast cancer. *Journal of Experimental & Clinical Cancer Research*, 32(1):32, 2013.

[125] H. K. Rooprai, A. Kandanearatchi, S. Maidment, M. Christidou, G. Trillo-Pazos, D. T. Dexter, G. Rucklidge, W. Widmer, and G. J. Pilkington. Evaluation of the effects of swainsonine, captopril, tangeretin and nobiletin on the biological behaviour of brain tumour cells in vitro. *Neuropathology and Applied Neurobiology*, 27(1):29–39, 2001.

[126] S. I. Rothschild and O. Gautschi. Src tyrosine kinase inhibitors in the treatment of lung cancer: rationale and clinical data. *Clinical Investigation*, 2(4):387–396, 2012.

[127] S. I. Rothschild, O. Gautschi, E. B. Haura, and F. M. Johnson. Src inhibitors in lung cancer: current status and future directions. *Clinical Lung Cancer*, 11(4):238–242, 2010.

[128] P. M. Rothwell, F. G. R. Fowkes, J. F. Belch, H. Ogawa, C. P. Warlow, and T. W. Meade. Effect of daily aspirin on long-term risk of death due to cancer: analysis of individual patient data from randomised trials. *The Lancet*, 377(9759):31–41, 2011.

[129] D. Rundle-Thiele, R. Head, L. Cosgrove, and J. H. Martin. Repurposing some older drugs that cross the blood–brain barrier and have potential anticancer activity to provide new treatment options for glioblastoma. *British Journal of Clinical Pharmacology*, 81(2):199–209, 2016.

[130] J. N. Sarkaria, P. Schwingler, S. E. Schild, P. T. Grogan, A. C. Mladek, S. J. Mandrekar, A. D. Tan, T. Kobayashi, R. S. Marks, H. Kita, et al. Phase i trial of sirolimus combined with radiation and cisplatin in non-small cell lung cancer. *Journal of Thoracic Oncology*, 2(8):751–757, 2007.

[131] H. Sasaki, M. Shitara, K. Yokota, Y. Hikosaka, S. Moriyama, M. Yano, and Y. Fujii. Increased fgfr1 copy number in lung squamous cell carcinomas. *Molecular Medicine Reports*, 5(3):725–728, 2012.

[132] R. Savai, S. S. Pullamsetti, G.-A. Banat, N. Weissmann, H. A. Ghofrani, F. Grimminger, and R. T. Schermuly. Targeting cancer with phosphodiesterase inhibitors. *Expert Opinion on Investigational Drugs*, 19(1):117–131, 2010.

[133] S. A. Selamat, B. S. Chung, L. Girard, W. Zhang, Y. Zhang, M. Campan, K. D. Siegmund, M. N. Koss, J. A. Hagen, W. L. Lam, et al. Genome-scale analysis of DNA methylation in lung adenocarcinoma and integration with mRNA expression. *Genome Research*, 22(7):1197–1211, 2012.

[134] N. Sharma, S. Thomas, E. B. Golden, F. M. Hofman, T. C. Chen, N. A. Petasis, A. H. Schönthal, and S. G. Louie. Inhibition of autophagy and induction of breast cancer cell death by mefloquine, an antimalarial agent. *Cancer Letters*, 326(2):143–154, 2012.

[135] C. Skriver, C. Dehlendorff, M. Borre, K. Brasso, H. T. Sørensen, J. Hallas, S. B. Larsen, A. Tjønneland, and S. Friis. Low-dose aspirin or other nonsteroidal anti-inflammatory drug use and prostate cancer risk: a nationwide study. *Cancer Causes & Control*, 27(9):1067–1079, 2016.

[136] G. Smyth. Limma: linear models for microarray data. in: Bioinformatics and computational biology solutions using R and Bioconductor'.(Eds r Gentleman, V Carey, S Dudoit, R Irizarry, W Huber) pp. 397–420, 2005.

[137] M. Socinski, S. Novello, J. Sanchez, J. Brahmer, R. Govindan, C. Belani, J. Atkins, H. Gillenwater, C. Palleres, and R. Chao. Efficacy and safety of sunitinib in previously treated, advanced non-small cell lung cancer (nsclc):

Preliminary results of a multicenter phase ii trial. *Journal of Clinical Oncology*, 24(18_suppl):7001–7001, 2006.

[138] J.-C. Soria, F. Shepherd, J.-Y. Douillard, J. Wolf, G. Giaccone, L. Crino, F. Cappuzzo, S. Sharma, S. Gross, S. Dimitrijevic, et al. Efficacy of everolimus (RAD001) in patients with advanced NSCLC previously treated with chemotherapy alone or with chemotherapy and EGFR inhibitors. *Annals of Oncology*, 20(10):1674–1681, 2009.

[139] H. Soule, J. Vazquez, A. Long, S. Albert, and M. Brennan. A human cell line from a pleural effusion derived from a breast carcinoma. *Journal of the National Cancer Institute*, 51(5):1409–1416, 1973.

[140] P. Stopfer, K. Rathgen, D. Bischoff, S. Lüdtke, K. Marzin, R. Kaiser, K. Wagner, and T. Ebner. Pharmacokinetics and metabolism of BIBF 1120 after oral dosing to healthy male volunteers. *Xenobiotica*, 41(4):297–311, 2011.

[141] Y. Sun, X. Lin, and H. Chang. Proliferation inhibition and apoptosis of breast cancer mcf-7 cells under the influence of colchicine. *J. BUON*, 3:570–575, 2016.

[142] L. M. Sutton, M. A. Warmuth, W. P. Petros, and E. P. Winer. Pharmacokinetics and clinical impact of all-trans retinoic acid in metastatic breast cancer: a phase ii trial. *Cancer Chemotherapy and Pharmacology*, 40(4):335–341, 1997.

[143] N. Takai and H. Narahara. Preclinical studies of chemotherapy using histone deacetylase inhibitors in endometrial cancer. *Obstetrics and Gynecology international*, 2010, 2010.

[144] T. Takeuchi, S. Tomida, Y. Yatabe, T. Kosaka, H. Osada, K. Yanagisawa, T. Mitsudomi, and T. Takahashi. Expression profile–defined classification of lung adenocarcinoma shows close relationship with underlying major genetic changes and clinicopathologic behaviors. *Journal of Clinical Oncology*, 24(11):1679–1688, 2006.

[145] K. Tandon, F. Herrmann, E. Ayaub, P. Parthasarathy, M. Ackermann, M. D. Inman, M. R. Kolb, L. Wollin, and K. Ask. Nintedanib attenuates the polarization of profibrotic macrophages through the inhibition of tyrosine phosphorylation on csf1 receptor. In *A72. MECHANISMS DRIVING FIBROSIS*, pages A2397–A2397. Am Thoracic Soc, 2017.

[146] C. Tekle, E. Giovannetti, J. Sigmond, J. Graff, K. Smid, and G. Peters. Molecular pathways involved in the synergistic interaction of the pkcβ inhibitor enzastaurin with the antifolate pemetrexed in non-small cell lung cancer cells. *British Journal of Cancer*, 99(5):750–759, 2008.

[147] A. Thomas, S. V. Liu, D. S. Subramaniam, and G. Giaccone. Refining the treatment of NSCLC according to histological and molecular subtypes. *Nature Reviews Clinical Oncology*, 12(9):511–526, 2015.

[148] J. Vansteenkiste, B. Solomon, M. Boyer, J. Wolf, N. Miller, L. Di Scala, I. Pylvaenaeinen, K. Petrovic, S. Dimitrijevic, B. Anrys, et al. Everolimus in combination with pemetrexed in patients with advanced non-small cell lung cancer previously treated with chemotherapy: a phase i study using a novel, adaptive bayesian dose-escalation model. *Journal of Thoracic Oncology*, 6(12):2120–2129, 2011.

[149] D. M. Vigushin, S. Ali, P. E. Pace, N. Mirsaidi, K. Ito, I. Adcock, and R. C. Coombes. Trichostatin a is a histone deacetylase inhibitor with potent antitumor activity against breast cancer in vivo. *Clinical Cancer Research*, 7(4):971–976, 2001.

[150] T. A. Wallace, R. L. Prueitt, M. Yi, T. M. Howe, J. W. Gillespie, H. G. Yfantis, R. M. Stephens, N. E. Caporaso, C. A. Loffredo, and S. Ambs. Tumor immunobiological differences in prostate cancer between African-American and European-American men. *Cancer Research*, 68(3):927–936, 2008.

[151] C. A. Walsh, J. C. Bolger, C. Byrne, S. Cocchiglia, Y. Hao, A. Fagan, L. Qin, A. Cahalin, D. McCartan, M. McIlroy, et al. Global gene repression by the steroid receptor coactivator SRC-1 promotes oncogenesis. *Cancer Research*, 74(9):2533–2544, 2014.

[152] S. N. Waqar, P. K. Gopalan, K. Williams, S. Devarakonda, and R. Govindan. A phase I trial of sunitinib and rapamycin in patients with advanced non-small cell lung cancer. *Chemotherapy*, 59(1):8–13, 2013.

[153] C.-C. Wen, H.-M. Chen, S.-S. Chen, L.-T. Huang, W.-T. Chang, W.-C. Wei, L.-C. Chou, P. Arulselvan, J.-B. Wu, S.-C. Kuo, et al. Specific microtubule-depolymerizing agents augment efficacy of dendritic cell-based cancer vaccines. *Journal of Biomedical Science*, 18(1):44, 2011.

[154] D. S. Wishart, C. Knox, A. C. Guo, S. Shrivastava, M. Hassanali, P. Stothard, Z. Chang, and J. Woolsey. DrugBank: a comprehensive resource for in silico drug discovery and exploration. *Nucleic Acids Research*, 34(suppl 1):D668–D672, 2006.

[155] L. Wollin, E. Wex, A. Pautsch, G. Schnapp, K. E. Hostettler, S. Stowasser, and M. Kolb. Mode of action of nintedanib in the treatment of mocetinostat pulmonary fibrosis. *European Respiratory Journal*, 51:ERJ–01749, 2015.

[156] J. E. Wooldridge, C. M. Anderson, and M. C. Perry. Corticosteroids in advanced cancer. *Oncology (Williston Park, NY)*, 15(2):225–34, 2001.

[157] G. Yan, K. Graham, and S. Lanza-Jacoby. Curcumin enhances the anti-cancer effects of trichostatin a in breast cancer cells. *Molecular Carcinogenesis*, 52(5):404–411, 2013.

[158] K.-H. Yan, Y.-W. Lin, C.-H. Hsiao, Y.-C. Wen, K.-H. Lin, C.-C. Liu, M.-C. Hsieh, C.-J. Yao, M.-D. Yan, G.-M. Lai, S.-E. CHUANG, and L.-M. LEE. Mefloquine induces cell death in prostate cancer cells and provides a potential novel treatment strategy in vivo. *Oncology Letters*, 5(5):1567–1571, 2013.

[159] K.-H. Yan, C.-J. Yao, C.-H. Hsiao, K.-H. Lin, Y.-W. Lin, Y.-C. Wen, C.-C. Liu, M.-D. Yan, S.-E. Chuang, G.-M. Lai, et al. Mefloquine exerts anticancer activity in prostate cancer cells via ROS-mediated modulation of Akt, ERK, jnk and AMPK signaling. *Oncology Letters*, 5(5):1541–1545, 2013.

[160] X. Yang, A. T. Ferguson, S. J. Nass, D. L. Phillips, K. A. Butash, S. M. Wang, J. G. Herman, and N. E. Davidson. Transcriptional activation of estrogen receptor α in human breast cancer cells by histone deacetylase inhibition. *Cancer Research*, 60(24):6890–6894, 2000.

[161] T. Yasukagawa, Y. Niwa, S. Simizu, and K. Umezawa. Suppression of cellular invasion by glybenclamide through inhibited secretion of platelet-derived growth factor in ovarian clear cell carcinoma ES-2 cells. *FEBS Letters*, 586(10):1504–1509, 2012.

[162] M. A. Yıldırım, K.-I. Goh, M. E. Cusick, A.-L. Barabási, and M. Vidal. Drug-target network. *Nature Biotechnology*, 25(10):1119–1126, 2007.

[163] K. Yoshida, K. Kuwano, N. Hagimoto, K. Watanabe, T. Matsuba, M. Fujita, I. Inoshima, and N. Hara. MAP kinase activation and apoptosis in lung tissues from patients with idiopathic pulmonary fibrosis. *The Journal of Pathology*, 198(3):388–396, 2002.

[164] Y. P. Yu, D. Landsittel, L. Jing, J. Nelson, B. Ren, L. Liu, C. McDonald, R. Thomas, R. Dhir, S. Finkelstein, et al. Gene expression alterations in prostate cancer predicting tumor aggression and preceding development of malignancy. *Journal of Clinical Oncology*, 22(14):2790–2799, 2004.

[165] P. Yuan, L. Di, X. Zhang, M. Yan, D. Wan, L. Li, Y. Zhang, J. Cai, H. Dai, Q. Zhu, et al. Efficacy of oral etoposide in pretreated metastatic breast cancer: A multicenter phase 2 study. *Medicine*, 94(17), 2015.

[166] P. Yuan, B.-H. Xu, J.-Y. Wang, F. Ma, Y. Fan, Q. Li, and P. Zhang. Oral etoposide monotherapy is effective for metastatic breast cancer with heavy prior therapy. *Chinese Medical Journal*, 125(5):775–779, 2012.

[167] J. Zhang, S. Kalyankrishna, M. Wislez, N. Thilaganathan, B. Saigal, W. Wei, L. Ma, I. I. Wistuba, F. M. Johnson, and J. M. Kurie. SRC-family kinases are activated in non-small cell lung cancer and promote the survival of epidermal growth factor receptor-dependent cell lines. *The American Journal of Pathology*, 170(1):366–376, 2007.